Acta Cryst. (1950). **3**, 436

The Crystal Structure of Decaborane, $B_{10}H_{14}$

By J. S. Kasper, C. M. Lucht and D. Harker*

Knolls Research Laboratory, General Electric Company, Schenectady, New York, U.S.A.

(*Received* 13 *March* 1950)

The crystal structure of decaborane has been determined from X-ray diffraction data. Crystals prepared by sublimation at room temperature, or above, show a high degree of polysynthetic twinning, giving rise to diffuseness of reflections for which h and k are odd. In the untwinned condition, the crystal is monoclinic, but pseudo-orthorhombic, and it is convenient to choose the twofold axis in the **c** direction. The space group is then $C112/a\text{–}C_{2h}^{4}$. With $a_0 = 14{\cdot}45$, $b_0 = 20{\cdot}88$, $c_0 = 5{\cdot}68$ A., $\beta = 90{\cdot}0°$, the cell contains 8 molecules of $B_{10}H_{14}$ and the calculated density is 0·96 g.cm.$^{-3}$.

The individual crystals that make up the actual, highly twinned crystalline edifice are so short in the **b** direction (a few unit translations) that it is convenient to consider the system as a partially ordered crystal, the disordered state of which is described by a unit cell one-quarter the size of the one mentioned above. The dimensions of this small cell are $a_0' = 7{\cdot}225$, $b_0' = 10{\cdot}44$, $c_0' = 5{\cdot}68$ A., and it contains $2B_{10}H_{14}$ or $(\frac{1}{2}B)_{20}(\frac{1}{2}H)_{28}$. The disordered structure based on this cell explains all the sharp spots observed—its space group is $Pnnm\text{–}D_{2h}^{12}$.

The solution of the structure resulted from a successful application of phase inequalities in obtaining an approximate projected structure (on (001)). The application of the inequalities is discussed in some detail.

The refinement of parameters has been accomplished by means of Fourier methods, including several three-dimensional syntheses. Hydrogen atoms are resolved, and all 14 of them in the molecule have been located from the electron-density maps.

The molecule is required by the space group to have only a twofold axis but appears to have two mirror planes as well; it has the symmetry $mm2$. The boron atoms are at 10 of the vertices of a somewhat distorted regular icosahedron, two neighboring vertices of which are unoccupied. The resulting arrangement forms two regular pentagonal pyramids with a common base edge. The angle between the base planes of those pyramids is 76°. Each of 10 hydrogen atoms is attached to a single boron atom in the direction of a fivefold axis of the icosahedron. The remaining four hydrogens *each bridge two boron atoms*. This structure is interpreted in terms of resonating single bonds, such as used by Pauling in describing metallic binding.

Introduction

One of the foremost unsolved problems of modern structural chemistry is that of the structures of the boron hydrides. The increasing interest in these compounds and in their peculiar properties, makes all the more desirable, at this time, any definitive structural information in this field. Most of the extensive literature pertaining to the structures of boron hydrides has been, perforce, speculative in character.

It is noteworthy, in this connection, that no recent X-ray studies of these compounds have been reported, despite the remarkable progress that has been made in structure determinations using X-ray diffraction effects. Altogether only three X-ray investigations have appeared in the literature (Mark & Pohland, 1925; Möller, 1931; Stock & Pohland, 1928). Apart from the relative scarcity of material, this situation is due also to the fact that only one member of this series of compounds, decaborane, is solid at room temperature. Möller (1931) was successful in obtaining good diffraction patterns from single crystals of decaborane, but he was unable to deduce the structure. Furthermore, his findings led to the improbable conclusion that two molecules of $B_{10}H_{14}$ are closely associated in the crystal.

Consequently, we deemed it highly important to undertake a complete crystal-structure determination for $B_{10}H_{14}$ when single crystals of this substance were made available to us.

Preliminary experimental results

The crystals of decaborane used in this investigation, and the physical data, were kindly provided for us by Dr Arthur E. Newkirk and other members of the Chemical Division of this laboratory. Clear, colorless needles or columns of $B_{10}H_{14}$, ranging in length from 0·5 mm. to 3 cm., were prepared by polymerization of lower-molecular-weight boron hydrides. These crystals were resublimed and then found to melt at 99·3° C. in agreement with the reported melting-point (Stock & Pohland, 1928).

Decaborane, unlike the other boron hydrides, is quite stable in air at room temperature, with respect to both oxidation and hydrolysis. However, its volatility presented a problem in obtaining satisfactory diffraction patterns—unprotected crystals were found to disappear in the X-ray beam during a short exposure. Enclosure

---

* Present address: The Protein Structure Project, Polytechnic Institute of Brooklyn, Brooklyn 2, N.Y., U.S.A.

of a crystal in a glass capillary was unsatisfactory owing to sublimation of the crystal and recrystallization within the capillary. This problem was solved most successfully, finally, by enclosing a crystal in a protective envelope of formvar film as described by Roth & Harker (1948). Not only was the crystal then preserved indefinitely in a fixed position, but also clear X-ray diffraction photographs (with extremely small background scattering) could be obtained with relatively short exposure times.

The preliminary investigations with X-rays soon revealed the all-important fact, not mentioned by Möller, that the crystals of decaborane are intimately twinned on a micro-crystalline scale, as evidenced by the diffuseness of certain reflections. On the other hand, all our other findings were in complete agreement with those of Möller, indicating that our crystals were the same as his. Thus, Laue photographs, taken with Mo and Cr radiations, showed orthorhombic symmetry, and rotation photographs about each of the principal axes gave the following unit-cell dimensions:

$$a_0 = 14{\cdot}45,\quad b_0 = 20{\cdot}88,\quad c_0 = 5{\cdot}68\,\text{A}.$$

The indexing of the reflections on the basis of this unit cell led to the same systematic extinctions as reported by Möller. The criteria were:

(1) hkl present only for $h+k=2n$,
(2) $hk0$ present only for $h=2n$, $k=2n$,
(3) $h0l$ present only for $\frac{1}{2}h+l=2n$,
(4) $0kl$ present only for $\frac{1}{2}k+l=2n$.

It is to be noted that conditions (3) and (4) are not required by any space group.

Also, all the intensity data given in Möller's article (mainly for the prism reflections) were in excellent agreement with our values. From the experimental density of 0·94 g.cm.$^{-3}$, we, too, decided that there are 8 molecules in the unit cell (calculated 7·93).

Our conclusion, then, would be identical with that of Möller—that the space group is D_{2h}^{21}-*Cmma*—were it not for the significant feature that *all reflections are diffuse for which h and k are both odd.* The nature of this diffuseness is such as to give maximum intensity at the reciprocal-lattice points but with a streaking only in the **b*** direction. This is most strikingly illustrated in rotation and oscillation photographs about the **b** axis, as in Fig. 1. All crystals of decaborane which we have examined (all at room temperature) have shown this diffuseness to the same degree for those reflections with h and k both odd. A logical explanation of both the diffuseness, just mentioned, and the non-space-group absences has led us to conclusions not in accord with Möller's.

Our first concern in this investigation was with the physical basis of the diffuse reflections.

Our diffraction data were obtained principally from four complete sets of oscillation photographs taken with Co $K\alpha$ radiation (filtered by iron foil)

$$(\lambda(\text{Co } K\alpha_{1,2}) = 1{\cdot}7902\,\text{A.}).$$

The axes of oscillation and the range of oscillation per film were:

a axis (15°); **b** axis (22·5°);
c axis (7·5°); (**a**+**b**) axis (22·5°).

In each case the overlap was one-third of the angular range. The full sphere of reflection was effectively covered thereby. The crystals were needles ranging in length from 0·5 to 1·0 mm. and in thickness from 0·2 to 0·3 mm.

The intensity of each reflection was estimated visually by comparison with a scale of intensities from 1 to 100, on an arbitrary basis. Since the exposure time, the crystal size, and other variables were not completely uniform, film factors were evaluated from comparisons of intensities of reflections occurring on two or more photographs. Having chosen one film as a standard, we were then able to record the intensities of all reflections on a comparable basis, by the application of the film factors. The final values for the intensities obtained by this process were judged to be precise to about ±20 %. Values of F^2_{hkl} (on an arbitrary scale) were then calculated from these intensities (I_{hkl}) by application of the Lorentz and polarization factors (*Internationale Tabellen...* (1935), vol. 2, p. 567). No correction was made, nor deemed necessary, for absorption.

In the case of the diffuse reflections, the maximum intensity at the reciprocal-lattice point was recorded for each such reflection.

The order–disorder phenomenon

Considering the reciprocal-lattice representation of the diffraction effects (Fig. 3), the rod-like streaks in the **b*** direction clearly indicate a failing in the periodicity of atomic arrangement in the **b** directions of the crystal. The very special nature of the streaking—only through select points (h and k both odd)—suggests further that there is no gross defect of structure such as irregularity in interplanar spacings. Instead, the diffuse streaking appears to result from a variation along the **b** direction

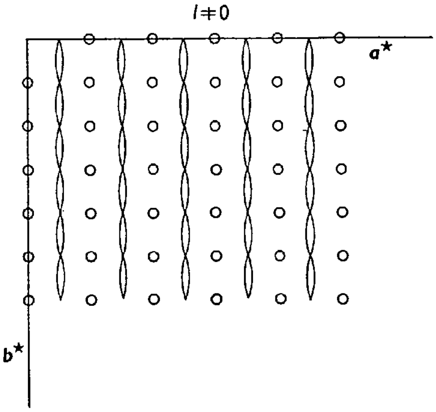

Fig. 3. Schematic reciprocal-lattice layer, illustrating diffuse streaking in the **b*** direction through lattice points for which h and k are both odd.

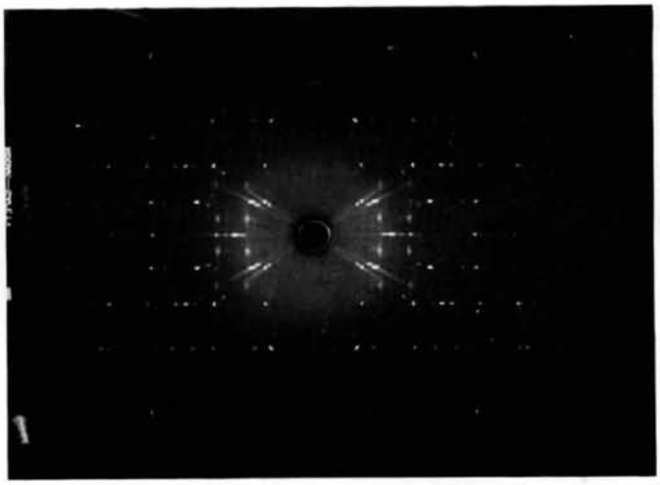

Fig. 1. Rotating-crystal photograph of $B_{10}H_{14}$, taken with Co unfiltered radiation. Rotation axis is **b**. Note the streaking in the **b*** direction for reflections on odd layers.

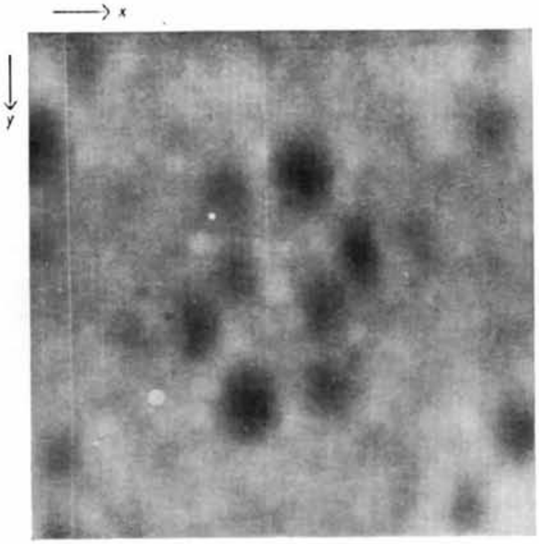

Fig. 2. Optical projection $\rho_z(x', y')$ showing the projected boron framework of the molecule.

in the periodicity of the orientation of molecules in the crystal.

The exact nature of the irregularities of structure could not be elucidated at this stage, of course, with no knowledge of the ideal structure. However, from these considerations of the diffraction effects, it was found convenient to regard the problem as a special type of order–disorder phenomenon. At room temperatures, then, decaborane is partially disordered. Since it was not possible to obtain a crystal with complete order, it was decided to attempt first the solution of the *completely disordered* structure, from which only the sharp reflections would be obtained. In principle, this latter situation could be a physical reality at more elevated temperatures.

The space groups of decaborane

From the data already given and the recognition of the order–disorder phenomena, it was possible to obtain the true space group, first for the disordered crystal, and then for the one with complete order.

Reviewing, in the light of the new findings, the criteria (p. 437) for the presence of spectra, we see that the only information that can be deduced from them alone is that the cell of the ordered structure is C-centered (criterion (1)) and that an a glide (perpendicular to **c**) is present (criterion (2)). We can summarize this in the symbols $C--a$, the dashes implying that the proper symmetries here are unknown.

For the description of the disordered structure, a cell only one-quarter the volume of that of the ordered one is necessary, resulting from halving both the a_0 and b_0 of the latter. The criteria for the occurrence of the spectra (sharp reflections only) then become:

$h'k'l'$ present for all cases,
$h'k'0$ present for all cases,
$h'0l'$ present only for $h'+l'=2n$,
$0k'l'$ present only for $k'+l'=2n$,

where $h'=\frac{1}{2}h$, $k'=\frac{1}{2}k$, $l'=l$, hkl being the indices for the large cell. The crystal system is orthorhombic and the space group from these criteria is either Pnn or $Pnnm$. Since an a glide (perpendicular to **c**) must be present in the large ordered cell, a mirror plane perpendicular to **c** is called for in the small cell. This follows from the principles for obtaining derivative structures, as given by Buerger (1947). The space group for the disordered structure is then $Pnnm$.

Further application of the same principles of derivative structures (Buerger, 1947) allows the determination of the space group for the ordered structure. In order to obtain the C-centered cell of twice the dimensions for a_0 and b_0, from the small cell with space group $Pnnm$, we find that the space group must be $C112/a$, a subgroup of $Cmma$, the one reported by Möller. The ordered structure is then *monoclinic*, and with monoclinic axes in the conventional orientation the description would be $P2/c\text{–}C_{2h}^4$. For convenience, however, we shall retain the orthorhombic axes for the ordered structure.

Accordingly, the appropriate descriptions for the two cases are:

Ordered structure	Disordered structure
Monoclinic	Orthorhombic
$a_0=14{\cdot}45$ A.	$a_0'=7{\cdot}225$ A.
$b_0=20{\cdot}88$ A.	$b_0'=10{\cdot}44$ A.
$c_0=5{\cdot}68$ A.	$c_0=5{\cdot}68$ A.
Space group $C112/a\text{–}C_{2h}^4$	Space group $Pnnm\text{–}D_{2h}^{12}$
$Z=8B_{10}H_{14}$	$Z=2\,(\frac{1}{2}B)_{20}(\frac{1}{2}H)_{28}$

The designation, $Z=2\,(\frac{1}{2}B)_{20}(\frac{1}{2}H)_{28}$, requires some explanation. In the small cell of the disordered structure there is the *equivalent* of two molecules of $B_{10}H_{14}$ (as determined from the density), but with twice the number of atomic positions required for two molecules. For complete disorder, the molecule occupies with equal probability either one set of positions, or another set related to the first by a mirror plane perpendicular to **c**. For purposes of analyzing the diffraction data, it is convenient to express this situation by considering $\frac{1}{2}$B (half the scattering factor of a boron atom) and $\frac{1}{2}$ H to be at each of the atomic positions provided by the space group $Pnnm$. Thus, for each $\frac{1}{2}$ B at x, y, z, there will be $\frac{1}{2}$ B at $x, y, \bar{z}$. A special feature to note is that the principal projections, on the (100), (010) and (001) faces, are identical for both the ordered and the disordered structures.

Solution of the disordered structure

In the absence of prior definite evidence for the structure of the decaborane molecule and of the structural principles for the boron hydrides, it seemed especially desirable to avoid a process of trial and error with the many structures that have been postulated. Accordingly, our first attempts to obtain the approximate structure were mainly through the use of Patterson and Patterson–Harker functions. Numerous such functions were evaluated and considerable effort was expended in their interpretation, but without success. A characteristic feature of these functions was the presence of many peaks, all of approximately the same height and often with poor resolution. In consideration of the many interatomic vectors that could be expected for a molecule of $B_{10}H_{14}$, this situation is not too surprising. The problem of interpretation was considerably more difficult than usual, also, because of the lack of a stereochemical basis for the structure of the molecule.

A large number of tests were made of postulated structures, not only as to their compatibility with the Patterson and Patterson–Harker functions, but on a trial-and-error basis of agreement between observed and calculated intensities. These latter attempts were without success, too, but it did appear unlikely to us that any of the structures in the literature was valid.

The first clue to the correct approximate structure resulted from a direct use of Fourier series for a projection on the (001) face, after the signs of a sufficient number of F_{hk0}'s were obtained through the use of phase-inequality relationships (Harker & Kasper, 1948; Gillis, 1948*a*, *b*).

Application of the inequality relationships

It is essential in the method of inequalities that the intensities be expressed in absolute units, i.e. that the F's be given as numbers of electrons (Harker & Kasper, 1948). We had not made any experimental measurements of absolute intensity, and relied instead on analytical methods for establishing an approximately 'absolute' scale.

One plausible method depends on the investigation of minima in the three-dimensional Patterson function. The argument is that the lowest minimum in Patterson space, occurring in a region which does not contain interatomic vectors, can be taken to be of value zero (when all F^2_{hkl}, including F^2_{000}, are in absolute units). For such a point (u_0, v_0, w_0), then

$$P(u_0, v_0, w_0) = 0 = F^2_{000} + \sum_{hkl} F^2_{hkl} \cos 2\pi(hu_0 + kv_0 + lw_0).$$

Accordingly, if F'^2_{hkl} represents the F^2_{hkl} value on an arbitrary scale, and C is a constant,

$$C \sum_{hkl} F'^2_{hkl} \cos 2\pi(hu_0 + kv_0 + lw_0) = -F^2_{000}.$$

The constant C can thus be evaluated and then used to convert the F^2 to an 'absolute' basis $(F^2_{hkl} = CF'^2_{hkl})$.

In the first application of the inequality relations, following their discovery, the scheme just described was used for expressing the F's in terms of electrons in order to obtain the quantities* $U_{hkl} = F_{hkl}/Z\hat{f}$ and U^2_{hkl} (where Z is the total number of electrons in the unit cell and $\hat{f}$ is the 'unitary atomic scattering factor' (Harker & Kasper, 1948)). With these values of U_{hkl} and U^2_{hkl} about one-third of the signs of F_{hk0}'s were at first obtained from the inequalities, but contradictions were then encountered, casting doubt on the process. It was realized then that the method of placing the intensities on an absolute basis was not satisfactory. For one thing, there was positive indication of the presence of a moderately large temperature factor but there was no means of allowing for it in the scheme. Consequently, as was found later, the magnitudes of U_{hkl} were generally too large for small values of $\sin\theta/\lambda$, and conversely.

Subsequently a sufficiently reliable method of placing the intensities on an absolute basis was worked out by one of us (Harker, 1948). (An almost identical treatment had been given by Wilson (1942), but was not known to us.) The substance of the method is that the mean value of U^2_{hkl} averaged over a large number of reflections, $\overline{U^2_{hkl}}$, is given by $\overline{U^2_{hkl}} = \sum_{j=1}^{N} n_j^2$, where $n_j = Z_j/Z$, the fraction of the electrons in the unit cell which belongs to the jth atom. If U'_{hkl} represents the quantity U computed with an arbitrary scale of intensities, then $U'_{hkl} = KU_{hkl}$ and $\overline{U'^2_{hkl}} = K^2 \sum_{j=1}^{N} n_j^2$. In the absence of thermal motion, K is a constant; otherwise K is a function of $\sin\theta/\lambda$ and may be expressed as

$$K = K_0 \exp[-B(\sin\theta/\lambda)^2].$$

The variation of K with $\sin\theta/\lambda$ can be obtained by taking narrow ranges of $\sin\theta/\lambda$ and performing the separate averages for reflections in each of these ranges. The values of U_{hkl} for $B_{10}H_{14}$ were then recomputed in this manner. Serious discrepancies were not encountered in the sign-determination process with this set of values.

The process of the sign determinations will be reviewed now in some detail. In Table 1 are listed the magnitudes of U_{hk0}, the signs of which it was desired to ascertain. (In this section, the indices are those appropriate to the small cell, i.e. $h'k'l'$. For typographical reasons the primes are omitted here.) Three separate groupings are made, since very frequently these groups function independently in the inequality relations. Table 2 contains both $|U_{hkl}|$ and U^2_{hkl} for those 'reflections' for which $|U_{hkl}| \geqslant 0{\cdot}30$, arranged in order of decreasing magnitude of U_{hkl}. (Also, included at the end of the table are a few reflections for which $|U_{hkl}| \leqslant 0{\cdot}30$, but which will be used in subsequent relations.)

The simplest inequality relations are those utilizing one symmetry element. Of the several separate elements of symmetry associated with the space group *Pnnm*, only the following were found to yield a definite sign determination:

m at $z=0$

$$2U^2_{hkl} \leqslant \{1 + U_{0,0,2l}\}, \qquad (1)$$

n at $y=\frac{1}{4}$

$$2U^2_{hkl} \leqslant \{1 + (-1)^{h+k+l} U_{0,2k,0}\}. \qquad (2)$$

For these relations to yield a sign determination it is necessary that the magnitude of the U on the right-hand side exceed that of $1 - 2U^2_{hkl}$. Accordingly, the comparison of these two terms is made in Table 3 with the resulting conclusion. Following Gillis (1948*b*), the sign of U_{hkl} will be indicated by the symbol S_{hkl}, which is either $+1$ or -1.

The last two entries in Table 3, while not establishing a sign, provide an illustration of the limitations which may be placed on an unobservable U_{hkl}, when hkl correspond to a reciprocal-lattice point beyond the sphere of reflection. Such information is often useful in allowing sign determinations with other inequalities, and frequent application of it will be made subsequently.

We next examine relations containing two separate

---

* For typographical reasons, we are adopting the change made by Gillis (1948*b*) in the symbol for the 'unitary structure factor', represented previously (Harker & Kasper, 1948; Gillis, 1948*a*) by $\hat{F}_{hkl}$.

Table 1. *Values of* $|U_{hk0}|$

$hk0$	$\|U_{hk0}\|$	$hk0$	$\|U_{hk0}\|$	$hk0$	$\|U_{hk0}\|$
800	0·42−	710	0·63−	670	0·59 (−)*
060	0·41−	570	0·53−	450	0·47+
080	0·39−	510	0·42 (+)*	290	0·47−
400	0·32+	550	0·35−	580	0·46−
420	0·31+	530	0·34+	180	0·45−
660	0·29−	190	0·30−	160	0·43−
040	0·28−	150	0·28−	340	0·40+
480	0·27−	330	0·22−	720	0·40+
220	0·27−	310	0·20−	360	0·38+
460	0·27−	110	0·19+	740	0·35+
0,10,0	0·26−	370	0·15+	270	0·31−
020	0·26+	130	0·14+	490	0·26−
260	0·24+	350	0·12+	470	0·25+
280	0·21+	750	0·11+	380	0·25+
240	0·21−	170	0	140	0·24−
200	0·19−	730	0	230	0·21+
600	0·10	390	0	630	0·20
620	0	590	0	540	0·20
440	0	1,11,0	0	410	0·19
640	0			430	0·17
2,10,0	0			520	0·15
4,10,0	0			810	0·14
				250	0·11+
				120	0·10
				210	0·09+
				320	0·04
				610	0
				650	0
				560	0
				1,10,0	0
				3,10,0	0
				2,11,0	0

* Assumed, see p. 443.

Table 2. $|U_{hkl}|$ *and* U^2_{hkl} *for reflections with* $|U_{hkl}| \geqslant 0{\cdot}30$*

hkl	$\|U_{hkl}\|$	U^2_{hkl}	hkl	$\|U_{hkl}\|$	U^2_{hkl}
710	0·63	0·40	351	0·37	0·14
701	0·61	0·37	134	0·36	0·13
670	0·59	0·35	352	0·36	0·13
544	0·58	0·34	324	0·36	0·13
206	0·56	0·31	501	0·36	0·13
570	0·53	0·28	461	0·35	0·12
006	0·52	0·27	004	0·35	0·12
226	0·52	0·27	522	0·35	0·12
643	0·52	0·27	550	0·35	0·12
450	0·47	0·22	293	0·35	0·12
423	0·47	0·22	740	0·35	0·12
290	0·47	0·22	443	0·34	0·12
105	0·46	0·21	530	0·34	0·12
580	0·46	0·21	133	0·34	0·12
180	0·45	0·20	322	0·34	0·12
171	0·45	0·20	412	0·33	0·11
561	0·44	0·19	172	0·33	0·11
015	0·43	0·19	521	0·33	0·11
160	0·43	0·19	073	0·33	0·11
510	0·42	0·18	234	0·33	0·11
144	0·42	0·18	400	0·32	0·11
281	0·42	0·18	262	0·32	0·11
800	0·42	0·18	553	0·32	0·11
060	0·41	0·17	333	0·32	0·11
340	0·40	0·16	313	0·32	0·11
720	0·40	0·16	062	0·32	0·11
080	0·39	0·15	270	0·31	0·10
432	0·39	0·15	124	0·31	0·10
360	0·38	0·14	420	0·31	0·10
204	0·38	0·14	153	0·30	0·09
033	0·38	0·14			
044	0·37	0·14	002	0·04	0·002
			202	0·11	0·001
			0,10,2	0	0
			604	0·26	0·068

* Also included are a few reflections for which $|U_{hkl}| \leqslant 0{\cdot}30$.

U's, corresponding to combinations of two symmetry elements. These are:

n at $x=\frac{1}{4}$, m at $z=0$

$$4U^2_{hkl} \leqslant \{1+(-1)^{h+k+l}\,U_{2h,0,0}\}\{1+U_{0,0,2l}\}, \qquad (3)$$

n at $y=\frac{1}{4}$, m at $z=0$

$$4U^2_{hkl} \leqslant \{1+(-1)^{h+k+l}\,U_{0,2k,0}\}\{1+U_{0,0,2l}\}, \qquad (4)$$

n at $x=\frac{1}{4}$, n at $y=\frac{1}{4}$

$$4U^2_{hkl} \leqslant \{1+(-1)^{h+k+l}\,U_{2h,0,0}\}\{1+(-1)^{h+k+l}\,U_{0,2k,0}\}. \qquad (5)$$

Table 3. *Results obtained from relations* (1) *and* (2)

Relation	*hkl*	$1\text{-}2U^2_{hkl}$	$\lvert U\rvert$	Conclusion
1	643	0·46	0·52	$S_{006}=+1$
2	544	0·32	0·39	$S_{080}=-1$
2	710	0·20	0·26	$S_{020}=+1$
2	570	0·44	—	$U_{0,14,0}\geqslant -0{\cdot}44$
2	670	0·30	—	$U_{0,14,0}\leqslant +0{\cdot}30$

Some of the results obtained with these relations are summarized in Table 4. The value of $4U^2_{hkl}$ is compared with that obtained for the right-hand side of the inequality for each of the four combinations of signs on the U's. These latter values are given in the four columns of Table 4 that are headed by a sign combination. Always, the first sign in the column heading refers to the first of the U's on the right-hand side of the inequality as written above.

To illustrate by example, the first entry of Table 4 (relation (5)) deals with the specific inequality, $4U^2_{423}\leqslant(1-U_{800})(1-U_{040})$ for which $4U^2_{423}$ is 0·88. Assuming the signs of both U_{800} and U_{040} to be +, one obtains 0·42 for the right side; assuming U_{800} to be + and U_{040} to be −, the value obtained is 0·74; etc. In order that the inequality be not violated, U_{080} cannot then be +.

The starred entries of Table 4 are cases where one of the U's is unknown, but where information as to sign can be obtained, notwithstanding. Here we assign the unknown U the value $+1$, -1 or 0, according to which makes the magnitude of the right side of the relation the largest. Sometimes, as for the first starred entry, the sign of an 'unobserved' U can be fixed ($S_{0,14,0}=+1$).

Limits on 'unobserved' U's can always be placed by these relations, and this is illustrated by Table 4 (*a*). Thus, using U^2_{701} and relation (3), together with the previously ascertained information that $S_{002}=+1$, we obtain that $U_{14,0,0}\geqslant +0{\cdot}42$. This can be used with U^2_{720} (relation (5)) to establish that $S_{040}=-1$.

We note here a contradiction regarding the sign of U_{040} (from Table 4, $S_{040}=+1$). This was the most serious error encountered. Further relations, to be discussed later, favored $S_{040}=-1$, and this value was used finally. It is quite important, therefore, that in the early stages, several independent sign determinations for a given U should be made, if possible.

For each of the relations (3), (4) or (5) with two symmetry elements, there is a companion relation obtained by a different application of Cauchy's inequality (Harker & Kasper, 1948). Thus, corresponding to relation (5) we have

$$4U^2_{hkl} \leqslant \{1+(-1)^{h+k+l}(U_{2h,0,0}+U_{0,2k,0})+U_{2h,2k,0}\}. \qquad (6)$$

Applying (6) then to $hkl=134$, for which $4U^2_{hkl}=0{\cdot}53$, we have

$$0{\cdot}53 \leqslant \{1+S_{200}(0{\cdot}19)+S_{060}(0{\cdot}41)+S_{260}(0{\cdot}24)\}.$$

Since $S_{060}=-1$ (Table 4),

$$0{\cdot}53 \leqslant \{0{\cdot}59+S_{200}(0{\cdot}19)+S_{260}(0{\cdot}24)\}.$$

We then conclude that S_{200} and S_{260} are not both -1.

Once a number of signs have been made available, it is then feasible to try the more complicated relations

Table 4. *Results obtained from relations* (3), (4) *and* (5)

Relation	*hkl*	$4U^2_{hkl}$	+ +	+ −	− +	− −	Conclusion
5	423	0·88	0·42	0·74	1·02	1·81	$S_{800}=-1$
3	423	0·88	0·89	0·28	2·15	0·68	$S_{006}=+1$
4	423	0·88	1·10	0·35	1·94	0·64	$S_{006}=+1$
5	450	0·88	0·43	0·73	1·05	1·79	$S_{800}=-1$
5	226	1·08	1·69	0·96	0·87	0·49	$S_{400}=+1$ ($S_{040}=+1$)
*5	710	1·60	2·52	1·48	1·26	0·74	$S_{020}=+1$, $S_{0,14,0}=+1$
*5	544	1·36	0·61	1·39	1·22	2·78	$S_{080}=-1$
5	234	0·44	0·40	0·96	0·78	1·87	If $S_{400}=+1$, $S_{060}=-1$
*3	643	1·08	1·52	0·48	3·04	0·96	$S_{006}=+1$
4	643	1·08	0·92	0·29	2·12	0·67	$S_{006}=+1$, $S_{080}=-1$
3	281	0·72	0·71	0·65	1·38	1·27	If $S_{400}=+1$, $S_{002}=+1$

* One U unknown.

Table 4 (*a*). *Limits on 'unobserved' U's*

	Relation			
	3	5	3	5
hkl	701	720	643	544
$4U^2_{hkl}$	1·48	0·64	1·08	1·36
+ +	$(1+\lvert U_{14,0,0}\rvert)\,(1{\cdot}04)$	0·43	$(1-\lvert U_{12,0,0}\rvert)\,(1{\cdot}52)$	—
+ −	$(1+\lvert U_{14,0,0}\rvert)\,(0{\cdot}96)$	0·77	—	$(1-\lvert U_{10,0,0}\rvert)\,(1{\cdot}39)$
− +	—	—	$(1+\lvert U_{12,0,0}\rvert)\,(1{\cdot}52)$	—
− −	—	—	—	$(1+\lvert U_{10,0,0}\rvert)\,(1{\cdot}39)$
Conclusion	$U_{14,0,0}\geqslant +0{\cdot}42$	$S_{040}=-1$	$U_{12,0,0}\leqslant +0{\cdot}29$	$U_{10,0,0}\leqslant 0{\cdot}05$

obtained from the structure-factor equation of the space group. For space group *Pnnm*, the unitary structure factor is either

$$U_{hkl}=8\sum_{j=1}^{\frac{1}{8}N} n_j\cos 2\pi hx_j\cos 2\pi ky_j\cos 2\pi lz_j$$

if $h+k+l$ is even,

or $$U_{hkl}=-8\sum_{j=1}^{\frac{1}{8}N} n_j\sin 2\pi hx_j\sin 2\pi ky_j\cos 2\pi lz_j$$

if $h+k+l$ is odd.

Depending on the choice of a_j in Cauchy's inequality,

$$\left|\sum_{j=1}^{N} a_jb_j\right|^2\leqslant\left(\sum_{j=1}^{N}|a_j|^2\right)\left(\sum_{j=1}^{N}|b_j|^2\right),$$

we can obtain the following three inequalities:

$$8U^2_{hkl}\leqslant\{1+U_{0,0,2l}\}\times\{1+U_{2h,2k,0}+(-1)^{h+k+l}(U_{2h,0,0}+U_{0,2k,0})\},\quad(7)$$

$$8U^2_{hkl}\leqslant\{1+(-1)^{h+k+l}U_{0,2k,0}\}\times\{1+U_{002l}+(-1)^{h+k+l}(U_{2h,0,0}+U_{2h,0,2l})\},\quad(8)$$

$$8U^2_{hkl}\leqslant\{1+(-1)^{h+k+l}U_{2h,0,0}\}\times\{1+U_{002l}+(-1)^{h+k+l}(U_{0,2k,0}+U_{0,2k,2l})\}.\quad(9)$$

For purposes of brevity we shall not discuss the application of these relations in detail. If the signs already determined and the magnitudes given in Tables 1 and 2 are inserted in the pertinent relations, the results expressed in Table 5 are obtained.

It is convenient at this point to summarize the signs already determined. They are:

hkl	*S*	*hkl*	*S*	*hkl*	*S*
200	−1	060	−1	420	+1
400	+1	080	−1	260	+1
800	−1	0,10,0	−1	202	−1
020	+1	002	+1	604	+1
040	−1	004	+1		
		006	+1		

So far the relations utilized have contained only U's for which *hkl* are all even. In order to get sign information for U_{hk0}'s where h, k are not both even, it is necessary to make use of 'addition–subtraction' relations, i.e. relations where two U's are added or subtracted before the application of Cauchy's inequality. The simplest such relation is

$$(U_{hkl}\pm U_{h'k'l'})^2\leqslant(1\pm U_{h+h',\,k+k',\,l+l'})\times(1\pm U_{h-h',\,k-k',\,l-l'}).\quad(10)$$

Extensive use of (10) was made by Gillis (1948*b*) in the application of inequalities for oxalic acid dihydrate, and we shall follow his scheme of expressing the results. These are given in Table 6.* The symbol H stands for *hkl*, H' for $h'k'l'$, $H+H'$ for $h+h',\ k+k',\ l+l'$, etc.

---

* It is to be noted that from the structure factors,

$$U_{hk0}=U_{h\bar{k}0}=U_{\bar{h}k0}=U_{\bar{h}\bar{k}0},\quad\text{if } h+k \text{ is even},$$

but that

$$U_{hk0}=-U_{h\bar{k}0}=-U_{\bar{h}k0}=U_{\bar{h}\bar{k}0},\quad\text{if } h+k \text{ is odd}.$$

Table 5. *Results obtained from relations* (7), (8) *and* (9)

Relation	*hkl*	$8U^2_{hkl}$	Result	Conclusion
9	351	1·09	0·86 if $S_{0\cdot10\cdot0}=+1$	$S_{0\cdot10\cdot0}=-1$
8	352	1·05	0·70 if $S_{004}=-1$ 0·88 if $S_{604}=-1$	$S_{004}=+1$ $S_{604}=+1$
7	216	0·38	0·22 if $S_{420}=-1$	$S_{420}=+1$
7	132	0·34	0·22 if S_{200} and S_{260} both −1	S_{200} and S_{260} not both −1
8	171	1·62	0·96 if $S_{200}=+1$ 1·12 if $S_{202}=+1$	$S_{200}=-1$ $S_{202}=-1$

Table 6. *Results obtained from relation* (11)

H	H'	$H+H'$	$H-H'$	+ +	+ −	− +	− −	Conclusion
006	200	206	206	$0·51\leqslant2·43$	—	—	0·19	$S_{206}=S_{200}\cdot S_{006}$ $=(-1)\,(+1)=-1$
206	020	226	226	$0·67\leqslant2·31$	—	—	0·23	$S_{226}=S_{206}\cdot S_{020}$ $=(-1)\,(+1)=-1$
006	220	226	226	$0·63\leqslant2·31$	—	—	0·23	$S_{226}=S_{006}\cdot S_{220}$ $-1=(+1)\,S_{220}$ $S_{220}=-1$
060	510	570	550	$0·69\leqslant2·06$	0·99	0·64	0·31	$S_{570}=S_{510}\cdot S_{060}$ $S_{570}=-S_{510}$
220	450	670	230	$0·55\leqslant1·91$	1·26	0·50	0·33	$S_{670}=S_{450}\cdot S_{220}$ $S_{670}=-S_{450}$
160	510	670	$4\bar{5}0$	$0·73\leqslant0·84$	2·34	0·22	0·61	$S_{670}=S_{160}\cdot S_{510}$
710	670	13,8,0*	$1\bar{6}0$	$1·49\leqslant1·14$	2·86	1·14	2·86	$S_{160}=-S_{710}\cdot S_{670}$
710	450	11,6,0*	$3\bar{4}0$	$1·22\leqslant1·18$	2·80	1·18	2·80	$S_{340}=-S_{710}\cdot S_{450}$
710	290	9,10,0*	$5\bar{8}0$	$1·22\leqslant1·08$	2·92	1·08	2·92	$S_{580}=-S_{710}\cdot S_{290}$
710	180	890*	$6\bar{7}0$	$1·18\leqslant0·82$	3·18	0·82	3·18	$S_{670}=-S_{710}\cdot S_{180}$
710	360	10,7,0*	$4\bar{5}0$	$1·03\leqslant1·06$	2·94	1·06	2·94	$S_{450}=-S_{710}\cdot S_{360}$ probably
040	510	550	530	$0·49\leqslant1·81$	0·89	0·87	0·43	Since $S_{040}=-1$, $S_{510}=S_{530}=S_{550}$ not allowed
020	550	570	530	$0·37\leqslant2·05$	1·01	0·63	0·31	Since $S_{020}=+1$, $S_{570}=S_{530}=-S_{550}$ not allowed

* Unobserved reflections which are given the values 0, +1 or −1, according as which makes the right-hand term of the inequality the largest.

In the next to last column, the quantity $(|U_H|+|U_{H'}|)^2$ is first given, then the four numbers for

$$\begin{gathered}(1+|U_{H+H'}|)(1+|U_{H-H'}|),\\ (1+|U_{H+H'}|)(1-|U_{H-H'}|),\\ (1-|U_{H+H'}|)(1+|U_{H-H'}|),\\ (1-|U_{H+H'}|)(1-|U_{H-H'}|),\end{gathered}$$

always in that order.

Relation (10) can be useful also when applied to U's for which the indices are all even, in which case it is possible to obtain a definite sign determination. Thus, the first three entries of Table 6 are for such a situation, and from them we have $S_{206}=S_{226}=S_{220}=-1$. On the other hand, where inequality (10) is applied to U's containing odd indices, relations only between the respective signs (S) can be obtained, such as $S_{570}=-S_{510}$. If an assumption is made as to the sign of one such U, then the signs for an entire group of U's are available. This assumption corresponds to a choice of origin among the several possible locations in the unit cell, and is, therefore, quite arbitrary. For the particular problem at hand, we are allowed two choices of sign for the U_{hk0}'s—one for a U_{hk0} with h, k both odd, and another choice for a U_{hk0} with either h odd, k even, or h even, k odd.

We first make the choice $S_{510}=+1$. The results of Table 6 then can be made to yield

$$\begin{aligned}&S_{570}=S_{710}=S_{550}=-1;\\ &S_{670}=S_{160}=S_{180}=-S_{450}=-S_{340}=-S_{360};\\ &S_{580}=S_{290}.\end{aligned}$$

There remains the other arbitrary choice of sign for one of the U_{hk0} with one of h, k odd. Choosing $S_{670}=-1$, we have

$$S_{670}=S_{160}=S_{180}=-S_{450}=-S_{340}=-S_{360}=-1$$

and $$S_{580}=S_{290}.$$

We turn now to more specialized relations. Limiting ourselves to those U_{hk0}'s for which $h+k$ is even (and for which, therefore,

$$U_{hk0}=8\sum_{j=1}^{\frac{1}{8}N} n_j\cos 2\pi hx_j\cos 2\pi ky_j),$$

if two such U's with a common index are added or subtracted before the application of Cauchy's inequality, a variety of new relations may be derived. Of these we shall find use for the following:

$$2(U_{hk0}\pm U_{h'k0})^2\leqslant\{1+U_{0,2k,0}\pm(U_{h+h',0,0}+U_{h+h',2k,0})\}\\ \times\{1\pm U_{h-h',0,0}\}, \tag{11}$$

$$2(U_{hk0}\pm U_{h'k0})^2\leqslant\{1+U_{0,2k,0}\}\\ \times\{1+\tfrac{1}{2}(U_{2h,0,0}+U_{2h',0,0})\pm(U_{h+h',0,0}+U_{h-h',0,0})\}, \tag{12}$$

$$2(U_{hk0}\pm U_{hk'0})^2\leqslant\{1+U_{2h,0,0}\}\\ \times\{1+\tfrac{1}{2}(U_{0,2k,0}+U_{0,2k',0})\pm(U_{0,k+k',0}+U_{0,k-k',0})\}. \tag{13}$$

Table 7 summarizes the results obtained from (11), (12) and (13). In each case H represents the indices of a U whose sign is known, and H' those of a U of unknown sign. Generally, at least one of the U's on the right-hand side of inequalities (11), (12) and (13) corresponds to an 'unobserved reflection', and for which information limiting its sign and magnitude is necessary. The information of this type used in each specific case is given in the last column, and the manner in which it was obtained is indicated at the bottom of Table 7.

Relations analogous to (11), (12) and (13) can be derived if the two U'_{hk0}'s that are added or subtracted are both with $h+k$ odd

$$\left(\text{for which } U_{hk0}=-8\sum_{j=1}^{\frac{1}{8}N} n_j\sin 2\pi hx_j\sin 2\pi ky_j\right).$$

We shall now utilize five such relations. They are:

$$2(U_{hk0}\pm U_{h'k0})^2\leqslant\{1-U_{0,2k,0}\}\\ \times\{1-\tfrac{1}{2}(U_{2h,0,0}+U_{2h',0,0})\mp(U_{h-h',0,0}-U_{h-h',0,0})\}, \tag{14}$$

$$2(U_{hk0}\pm U_{hk'0})^2\leqslant\{1-U_{2h,0,0}\}\\ \times\{1-\tfrac{1}{2}(U_{0,2k,0}-U_{0,2k',0})\mp(U_{0,k+k',0}-U_{0,k-k',0})\}, \tag{15}$$

$$2(U_{hk0}-U_{hk'0})^2\leqslant\{1+U_{0,k+k',0}\}\\ \times\{(1-U_{2h,0,0}-U_{0,k-k',0}+U_{2h,k-k',0})\}, \tag{16}$$

$$2(U_{hk0}+U_{hk'0})^2\leqslant\{1-U_{0,k+k',0}\}\\ \times\{(1-U_{2h,0,0}+U_{0,k-k',0}-U_{2h,k-k',0})\}, \tag{17}$$

$$2(U_{hk0}+U_{hk'0})^2\leqslant\{1-U_{2h,0,0}-U_{0,k+k',0}+U_{2h,k+k',0}\}\\ \times\{(1+U_{0,k-k',0})\}. \tag{18}$$

Table 7. *Results obtained from relations* (11)–(13)

Relation	H	H'	Result	Conclusion	Special information used
12	550	350	$0{\cdot}44\leqslant0{\cdot}36$ if $S_{350}=-1$	$S_{350}=+1$	$U_{10,0,0}\leqslant+0{\cdot}05$ (Table 4 (*a*))
13	550	530	$0{\cdot}95\leqslant0{\cdot}56$ if $S_{530}=-1$	$S_{530}=+1$	,,
12	510	310	$0{\cdot}77\leqslant0{\cdot}59$ if $S_{310}=+1$	$S_{310}=-1$	,,
12	530	330	$0{\cdot}63\leqslant0{\cdot}28$ if $S_{330}=+1$	$S_{330}=-1$	,,
12	530	130	$0{\cdot}46\leqslant0{\cdot}42$ if $S_{130}=-1$	$S_{130}=+1$	,,
12	570	370	$0{\cdot}92\leqslant0{\cdot}62$ if $S_{370}=-1$	$S_{370}=+1$	$U_{10,0,0}\leqslant+0{\cdot}05$ $U_{0,14,0}\leqslant+0{\cdot}32$
12	710	110	$1{\cdot}35\leqslant1{\cdot}15$ if $S_{110}=-1$	$S_{110}=+1$	$U_{14,0,0}\leqslant+0{\cdot}66$
13	110	190	$0{\cdot}48\leqslant0{\cdot}28$ if $S_{190}=+1$	$S_{190}=-1$	$U_{0,18,0}\leqslant-0{\cdot}29$
11	550	150	$0{\cdot}79\leqslant0{\cdot}78$ if $S_{150}=+1$	$S_{150}=-1$ probably	$U_{6,10,0}\geqslant-0{\cdot}32$
13	710	750	$1{\cdot}09\leqslant0{\cdot}62$ if $S_{750}=-1$	$S_{750}=+1$	—

Relation	Special information	Conclusion
5	$4U_{171}^2=0{\cdot}81\leqslant(1-U_{200})\ (1-U_{0,14,0})$	$U_{0,14,0}\leqslant+0{\cdot}32$
5	$4U_{290}^2=0{\cdot}88\leqslant(1-U_{400})\ (1-U_{0,18,0})$	$U_{0,18,0}\leqslant-0{\cdot}29$
5	$4U_{740}^2=0{\cdot}48\leqslant(1-U_{14,0,0})\ (1-U_{080})$	$U_{14,0,0}\leqslant+0{\cdot}66$
6	$4U_{352}^2=0{\cdot}52\leqslant(1+U_{600}+U_{0,10,0}+U_{6,10,0})$	$U_{6,10,0}\geqslant-0{\cdot}32$

It is to be noted that for the last five entries of Table 8, which summarizes the results from the use of the relations above, the difference of the two values in the inequality is well within the error to be expected for the method of inequalities. Lacking stronger criteria, we accept the signs indicated as being more probable than their opposites, especially since, in the relations used, the most adverse value for an 'unobserved' U has been employed. Generally, more than one such weak inequality can be obtained for the reflections in question, somewhat in support of the probability argument.

There remain a few U's with even indices whose signs are still unknown. We are in a position now to use more complicated relations for this purpose than previously, since a good number of signs of U's with odd indices have been established. We shall give only one such relation, derivable from the structure factor

$$U_{hk0} = 8 \sum_{j=1}^{\frac{1}{4}N} n_j \cos 2\pi h x_j \cos 2\pi k y_j, \quad h+k \text{ even},$$

$$\begin{aligned} 4(U_{hk0} \pm U_{h'k'0})^2 \leqslant (2 + U_{2h00} + U_{0,2k,0} + U_{2h,2k,0} \\ + U_{2h',2k',0}) \pm 2(U_{h+h',k+k',0} + U_{h+h',k-k',0} \\ + U_{h-h',k+k',0} + U_{h-h',k-k',0}). \qquad (19) \end{aligned}$$

The information obtained from the use of (19) is given in Table 9, along with the pertinent data.

For practical purposes, a convenient stopping point was now reached. A further search for signs which had not already been determined appeared to be a lengthy and complicated process, and in general would give no new result. Also, it seemed likely that sufficient signs were available now to proceed to a Fourier synthesis. The summary of the information obtained from the inequalities as to signs of U_{hk0}'s is included in Table 1. Ultimately, three of these, namely, S_{130}, S_{380}, S_{210}, were found to be wrong. However, two of these, S_{130} and S_{210}, changed sign only in the latter stages of refinement, when it was found necessary to include hydrogen parameters. In addition, we have also established a few signs for other than U_{hk0}'s. Thus, $S_{002} = +1$, $S_{004} = +1$, $S_{006} = +1$, $S_{202} = -1$, $S_{604} = +1$, $S_{206} = -1$, $S_{226} = -1$.

It should be mentioned that we have not given here a complete résumé of all the numerous trials with the many inequalities provided by the space group *Pnnm*. It has been our purpose to indicate as concisely as possible the method of operation with the inequalities, and to give at least one example of sign determination for each U_{hk0} whose sign was believed to be established.

Table 8. *Results obtained from relations* (14)–(18)

Relation	H	H'	Result	Conclusion	Special information needed
14	180	580	$1 \cdot 66 \leqslant 1 \cdot 16$ if $S_{580} = +1$	$S_{580} = -1$ $S_{290} = -1$	$U_{10,0,0} \geqslant 0 \cdot 21$ $S_{580} = S_{290}$
14	340	740	$1 \cdot 13 \leqslant 0 \cdot 79$ if $S_{740} = -1$	$S_{740} = +1$	$U_{14.0.0} \geqslant +0 \cdot 42$ (Table 4 (*a*)) $U_{10,0,0} \leqslant +0 \cdot 05$ (Table 4 (*a*))
15	740	720	$1 \cdot 13 \leqslant 0 \cdot 39$ if $S_{720} = -1$	$S_{720} = +1$	$U_{14.0.0} \geqslant +0 \cdot 42$ (Table 4 (*a*))
14	670	270	$1 \cdot 62 \leqslant 0 \cdot 60$ if $S_{270} = +1$	$S_{270} = -1$	$U_{0,14,0} \geqslant 0$ (Table 4)
14	180	380	$0 \cdot 98 \leqslant 0 \cdot 85$ if $S_{380} = -1$	$S_{380} = +1$	$U_{0,16,0} \geqslant -0 \cdot 33$
16	160	140	$0 \cdot 90 \leqslant 0 \cdot 49$ if $S_{140} = +1$	$S_{140} = -1$	—
15	290	230	$0 \cdot 93 \leqslant 0 \cdot 90$ if $S_{230} = -1$	$S_{230} = +1$ probably	$U_{0,18,0} \geqslant -0 \cdot 55$ $U_{0,12,0} \geqslant -0 \cdot 25$
15	290	210	$0 \cdot 65 \leqslant 0 \cdot 69$ if $S_{210} = -1$	$(S_{210} = -1)$ probably	$U_{0,18,0} \geqslant -0 \cdot 55$
10	710	470	$0 \cdot 77 \leqslant 0 \cdot 79$ if $S_{470} = -1$	$(S_{470} = +1)$ probably	$U_{11,8,0} \leqslant +0 \cdot 29$
17	450	490	$1 \cdot 06 \leqslant 1 \cdot 04$ if $S_{490} = +1$	$S_{490} = -1$ probably	$U_{0,14,0} \geqslant 0$ (Table 4) $U_{840} \geqslant +0 \cdot 10$
18	290	250	$0 \cdot 67 \leqslant 0 \cdot 64$ if $S_{250} = -1$	$S_{250} = +1$ probably	$U_{0,14,0} \geqslant 0$ (Table 4) $U_{4,14,0} \leqslant +0 \cdot 21$

Relation	Special information	Conclusion
5	$4U_{530}^2 = 0 \cdot 46 \leqslant (1 + U_{10,0,0})\ (1 + U_{060})$	$U_{10,0,0} \geqslant -0 \cdot 21$
10	$(U_{0,10,0} + U_{0,60})^2 \leqslant (1 + U_{0,16,0})^2$	$U_{0,16,0} \leqslant -0 \cdot 33$
5	$4U_{190}^2 = 0 \cdot 36 \leqslant (1 + U_{200})\ (1 + U_{0,18,0})$	$U_{0,18,0} \geqslant -0 \cdot 55$
4	$4U_{561}^2 = 0 \cdot 78 \leqslant (1 + U_{0,12,0})\ (1 + U_{002})$	$U_{0,12,0} \geqslant -0 \cdot 25$
10	$(U_{670} - U_{510})^2 \leqslant (1 - U_{11,8,0})\ (1 - U_{160})$	$U_{11,8,0} \leqslant +0 \cdot 29$
6	$4U_{420}^2 = 0 \cdot 40 \leqslant (1 + U_{800} + U_{040} + U_{840})$	$U_{840} \geqslant +0 \cdot 10$
10	$(U_{580} - U_{\bar{1}60})^2 \leqslant (1 - U_{4,14,0})\ (1 - U_{620})$	$U_{4,14,0} \leqslant +0 \cdot 21$

Table 9. *Results obtained from relation* (19)

Relation	H	H'	Result	Conclusion	Special information used
19	150	330	$1 \cdot 00 \leqslant 0 \cdot 65$ if $S_{280} = -1$	$S_{280} = +1$	—
19	400	080	$2 \cdot 01 \leqslant 0 \cdot 80$ if $S_{450} = +1$	$S_{480} = -1$	$U_{0,16,0} \leqslant 0$
19	400	060	$2 \cdot 13 \leqslant 1 \cdot 74$ if $S_{460} = +1$	$S_{460} = -1$	$U_{0,12,0} \leqslant +0 \cdot 37$
10	710	$6\bar{6}0$	$0 \cdot 87 \leqslant 0 \cdot 60$ if $S_{660} = +1$	$S_{660} = -1$	$U_{13,5,0} \geqslant +0 \cdot 40$
19	330	110	$1 \cdot 07 \leqslant 0 \cdot 69$ if $S_{240} = +1$	$S_{240} = -1$	—

Relation	Special information	Conclusion
5	$4U_{281}^2 = 0 \cdot 70 \leqslant (1 - U_{400})\ (1 - U_{0,16,0})$	$U_{0,16,0} \leqslant 0$
5	$4U_{160}^2 = 0 \cdot 75 \leqslant (1 - U_{200})\ (1 - U_{0,12,0})$	$U_{0,12,0} \leqslant +0 \cdot 37$
10	$(U_{670} + U_{7\bar{2}0})^2 \leqslant (1 + U_{13.5,0})\ (1 + U_{190})$	$U_{13,5,0} \geqslant +0 \cdot 40$

The projection on (001)

The signs for most of the U_{hk0}'s having now been provided, the direct Fourier synthesis of the projection on the (001) face was attempted. Since it could be anticipated that several trial syntheses would be required because not all the signs were known, it was especially desirable to have a rapid means of obtaining electron-density maps. The optical scheme developed by Huggins (1941) of the Eastman-Kodak Co. was found to be admirably satisfactory for this purpose. This scheme is a refinement of the procedure used originally by Bragg (1929), in which the electron density in the unit cell is produced on to a single photographic paper by means of successive exposures through a series of '*h k* masks'. One such mask contains alternating light and dark bands arranged so as to give a variation in transmitted light intensity in accordance with *one* term of the Fourier series, i.e. as $\cos 2\pi(hx+ky)$. The exposure time for a given mask is made proportional to the magnitude of the amplitude, $|F_{hk0}|$. Thus, a single exposure corresponds to a single term of the Fourier series. The masks prepared by Huggins* are very conveniently arranged in an orderly sequence on 35 mm. movie film. The film can be run through a device which allows to translate from one mask to the next by one motion of a crank. This device can be inserted in a photographic enlarger, and the time of exposure regulated by an automatic time controller. With such an arrangement, it was found that a projection of electron density containing 70 Fourier terms could be obtained in 1–1½ hr. The time taken for the same projection when calculated with a hand computing machine and using Beevers–Lipson strips was about one week, or using IBM machines and punched cards, about 4 hr.

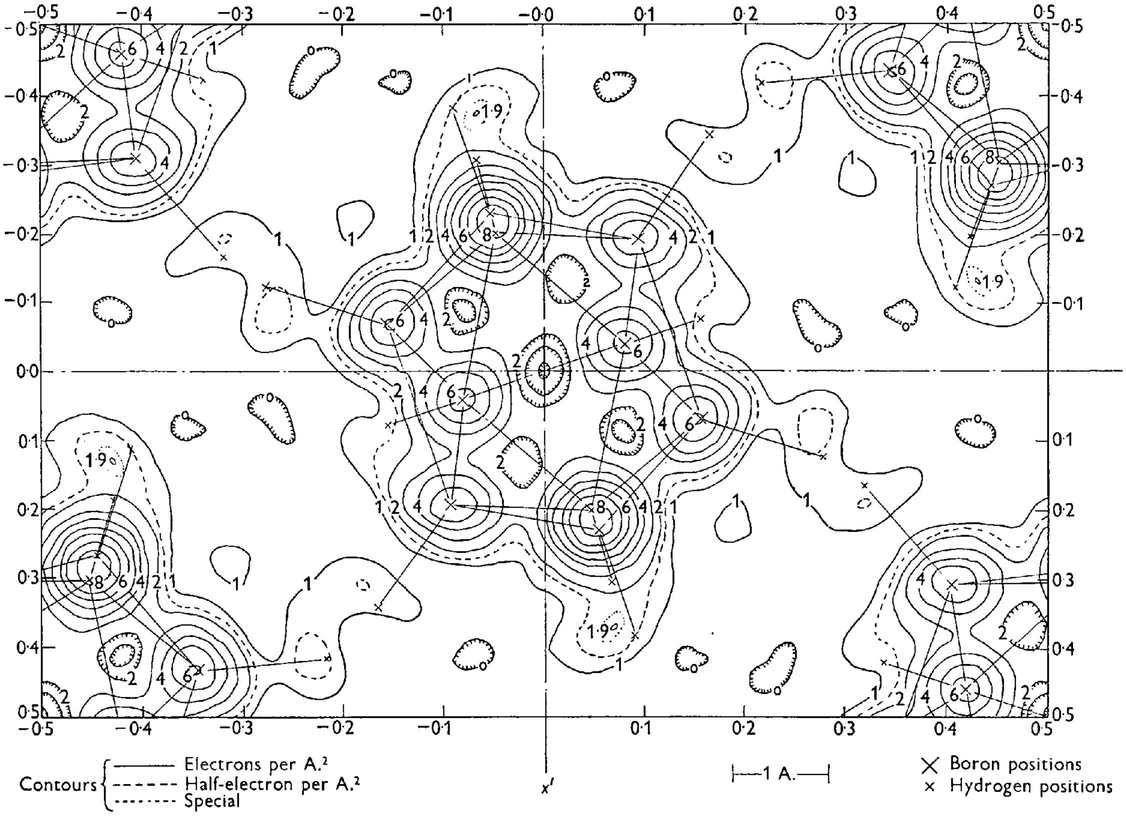

Fig. 4. Projection $\rho_z(x', y')$.

About a dozen trials were necessary to obtain the first satisfactory projection, $\rho_z(x', y')$, by the optical scheme, using the sign information discussed in the previous section. This projection is shown in Fig. 2, where the boron atoms of one molecule can be seen grouped centrosymmetrically about the center of the picture. Actually, only eight regions of high electron density are indicated, but two of these are much more intense (about twofold) than the others. These two regions were each taken to represent approximate superposition of two boron atoms. Thus, approximate x' and y' parameters were obtained for each of the boron atoms. These were, for the five boron atoms of the asymmetric unit of structure (one-half of the molecule), the following:

	x'	y'
B_I	0·067	0·150
B_{II}	0·208	0·054
B_{III}	0·232	0·060
B_{IV}	0·173	−0·087
B_V	0·039	−0·084

---

* We are gratefully indebted to Dr M. L. Huggins for providing us with a set of the masks.

The intensities of the $hk0$ reflections calculated from the parameters above were in sufficiently satisfactory agreement with the observed values to imply the validity of the projected structure and to suggest a refinement of the parameters by the usual means of successive computed Fourier syntheses. The final Fourier projection for $\rho_z(x', y')$ obtained by this process is shown in Fig. 4. A noteworthy feature of this projection is that, while only a center of symmetry for the projected structure is required by the Fourier series, two mirror planes, perpendicular to the x', y' plane, are indicated for the molecule. They correspond closely to the planes, $x' = +4y'$, and $y' = -2x'$. While the x' and y' co-ordinates of three boron atoms can be obtained readily, those of the other two are inaccurate because of superposition. It is seen, however, that the large peak corresponding to the overlap of the two atoms is elongated along one of the mirror planes ($x' = +4y'$). Consequently the x' and y' parameters for these two atoms were obtained from a comparison of observed and calculated $F_{h'k'0}$'s. This was treated as a one-parameter variation problem, since the two atoms were considered displaced symmetrically about the center of the Fourier peak along the line $x' = +4y'$. The parameters arrived at from the computed projection and the variation treatment were:

	x'	y'
B_I	0·067	0·157
B_{II}	0·198	0·047
B_{III}	0·238	0·057
B_{IV}	0·193	−0·096
B_V	0·038	−0·079

The molecular configuration

The first set of approximate z parameters for boron atoms, needed to outline the configuration of the molecule, was obtained mainly as the result of a fortunate guess for the molecular structure, which guess proved to be essentially correct in the ultimate analysis. It was based on considerations of expected interatomic distances for boron atoms (approximately 1·8 A.), of symmetry, and of the intensities for $h0l$ and $0kl$ reflections, as well as partial sign information. The following z values were thus obtained:

	z
B_I	0
B_{II}	0·167
B_{III}	−0·167
B_{IV}	0
B_V	0·23

It is not possible to define uniquely the molecular geometry with only the knowledge of the parameters above. For the disordered structure, where the asymmetric unit is repeated four times, it is immaterial whether any z parameter is taken positive or negative. On the other hand, the true molecular configuration corresponds to one of two possible pairings of the asymmetric unit—either by a twofold axis or by an inversion center. The former gives a 'cap' model for the molecule, the latter a 'crown' arrangement of the boron atoms. The choice could be made only from a consideration of the ordered structure—in this case, a comparison of observed and calculated intensities of the diffuse reflections. Such preliminary calculations of intensities (for details see the section on the ordered structure) were in satisfactory agreement with those observed for the 'cap model' and in marked disagreement for the 'crown model'.

Since in the disordered structure the molecule appears reflected through a mirror plane at $z = 0$, it is fortunate that the z parameters have these particular values, i.e. with them the molecule and its reflection coincide for four of the five boron atoms of the asymmetric unit. Only B_V does not superimpose on its reflected image, and it alone contributes mainly to the intensities of the diffuse reflections.

Actually, B_{II} and B_{III} do not reflect exactly into one another through $z = 0$ (cf. their x', y' parameters), and their z parameters would not be expected to be the same. Indeed, one of the main purposes of the subsequent refinement of parameters was to obtain the exact values for B_{II} and B_{III}.

As a check on the approximate z parameters, calculations of $F_{h'0l'}$ and $F_{0k'l'}$ were made and found to be in fair agreement in magnitude with the observed quantities. Also, the Fourier projections $\rho_{x'}(y', z)$ and $\rho_{y'}(x', z)$ were computed and found to be compatible with the assigned parameters. Because of the extensive overlapping of atoms in these projections, they were not used for refinement of z parameters, but instead three-dimensional syntheses were undertaken.

Three-dimensional syntheses

Better values for all boron parameters were obtained from the following Fourier sections: $\rho(x', y', 0)$, $\rho(x', -2x', z)$ and $\rho(+4y', y', z)$. (The last two sections are very close to the two mirror planes of symmetry of the molecule.) In addition, very definite indications of hydrogen positions were given, as evidenced by electron-density peaks of the proper magnitude. From these three sections, five of the seven hydrogens of the asymmetric unit were well resolved, the other two being in doubt. The appearance of the hydrogen atoms is shown in Fig. 5, the section $\rho(x', y', 0)$, where the four which are attached to B_I and B_{IV}, and B'_I and B'_{IV} (related by a twofold axis to B_I and B_{IV}) are indicated by the electron-density peaks which are above 0·5 e.A.$^{-3}$. It will be noted that in this section there are two regions of high electron density near the origin. These were also interpreted at one time as possible hydrogen positions, but shown to be spurious subsequently.

That electron-density peaks represented hydrogens was made reasonable by a recalculation of intensities, including parameters obtained for five hydrogens from the Fourier maps. For at least a dozen reflections very marked improvement in agreement was obtained by the inclusion of the hydrogen atoms. At this stage, the other two hydrogen positions were guessed*—erroneously it turned out—but their contributions to the intensities were generally not too significant.

It seemed quite essential in this problem to explore the electron-density distribution in the entire unit cell—both to check on hydrogen positions and to obtain the best parameter values for boron atoms. With regard to the last point, in working with the *disordered structure* there is the complication of overlapping atoms even in the three-dimensional syntheses. Accordingly, there was needed more than the usual concern with the details of electron-density maps—peak shape and height, magnitude of background fluctuations, etc. The three-dimensional exploration was accomplished by computing a series of parallel sections normal to **c**, i.e. $\rho(x', y', z_0)$, where z_0 was increased successively from 0 by $\frac{2}{60}$ths or a spacing of 0·19 A. Because of symmetry, the maximum value of z_0 needed was $\frac{1}{4}$ or $\frac{15}{60}$ths. In all, eight two-dimensional Fourier syntheses were calculated. Where needed, the values of the electron density for intermediate z's were obtained by interpolation.

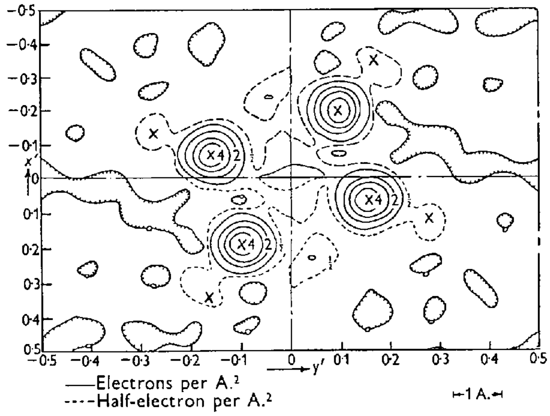

Fig. 5. Section $\rho(x', y', 0)$.

The computations were made with punched cards† and IBM machinery, according to a scheme similar to that described by Shaffer, Schomaker & Pauling (1946). The intervals of x' and y' were $\frac{1}{60}$ths or spacings of 0·12 and 0·17 A. respectively.

Before undertaking these calculations, the observed intensities were adjusted to a 'more absolute' scale by comparison with the calculated intensities. It was especially desirable to have true electron density represented in the Fourier plots.

The results of this investigation were very satisfactory in most respects. That the series had reached convergence was evidenced by the occurrence of the boron peak maxima at the same positions as previously determined and by no significant changes of sign upon recalculation of F's. The following important features were ascertained:

Boron positions

Despite lack of great precision in some of the z parameters, the molecular symmetry was definitely established as $mm2$. Thus, the four boron atoms B_I, B_{IV} and B'_I and B'_{IV} (section $\rho(x', y', 0)$, Fig. 5) form a perfect rectangle, though not required to do so by the Fourier series. Boron atoms B_V and B'_V lie exactly in one of the mirror planes of the molecule and B_{II}, B_{III} (also B'_{II} and B'_{III}) in the other mirror plane. This follows from the x' and y' parameters which were now quite accurate for all boron atoms.

The problem of overlapping of atoms resulting from the fact that in the disordered structure the molecule appears with its image reflected through the plane at $z = 0$, did not prove too troublesome. Thus, B_V and B'_V, which are the only two atoms that do not suffer from this difficulty, were well resolved, round in shape and with an electron density of 2·5 e.A.$^{-3}$, corresponding to $\frac{1}{2}$ B. Their z parameters, therefore, could be determined quite accurately. For B_I, B'_I, B_{IV}, B'_{IV}, the overlap seems to be perfect, judged from the shape of the atoms and the fact that their peak heights correspond to 5 or almost 5 e.A.$^{-3}$, or 2($\frac{1}{2}$ B). The z parameter for those four atoms could be fixed then at $z = 0$ ($z < 0·005$).

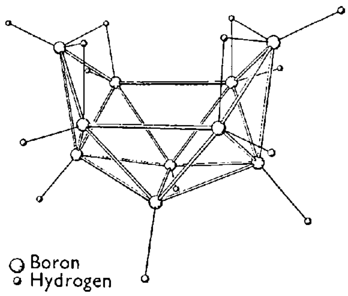

Fig. 6. Form of the molecule of $B_{10}H_{14}$.

On the other hand, it was not possible to obtain the accurate values of the z parameters of B_{II} and B_{III} from the contour maps. This resulted from the close, but not exact, overlap of B_{II} with B_{III} of the 'image' molecule and conversely. The centers, nonetheless, occurred on the mirror plane of the molecule, as found previously. Also, as before (see the projection, $\rho_z(x', y')$ Fig. 4), there was definite indication of two separate peaks merged together. Concomitantly with this phase of the work, calculations of intensities were made with a variation of the z parameters of B_{II} and B_{III}, both for the sharp reflections used in the series here and for the diffuse reflections—many of which are sensitive to these parameters. The best values arrived at on this basis were compatible with the density maps and are included in the final set of parameters (below). They are probably reliable to ±0·01 in z.

The resulting boron framework of the molecule can

---

* One of these guesses appears in a letter to the editor of the *Journal of the American Chemical Society* (Kasper, Lucht & Harker, 1948).

† We are very grateful to Dr V. Schomaker of the California Institute of Technology for a master set of the cards used in these calculations.

be described by saying that the boron atoms occupy ten of the twelve vertices of a distorted icosahedron (Fig. 6).

Hydrogen positions

The results of the three-dimensional syntheses with respect to hydrogen positions were most pleasing. It was possible to decide, at least approximately, the location of all 14 of them. Ten of them (H_I to H_V, H'_I to H'_V), located previously, may be considered as 'regular' and are bonded each to a single boron atom (H_I to B_I, etc.) at a distance of 1·2–1·3 A. They were somewhat better resolved than previously and attained a peak height between 0·6 and 1·2 e.A.$^{-3}$. The remaining four hydrogen atoms were found to be all of the same kind, each of them serving as an unsymmetrical bridge between two boron atoms. H_{VI} bridges B_I and B_{III}, while H_{VII} is between B_{III} and B_{IV}. These, also, had an electron density $>0·6$ e.A.$^{-3}$.

In addition to the fourteen peaks for the hydrogen positions, there persisted still the two of ~ 1 e.A.$^{-3}$ close to the origin and two others of almost 0·5 e.A.$^{-3}$. Although all of these were in what appeared as unlikely sites for hydrogen, their spurious nature was proven by computing several Fourier series in which the F values used were *those computed from the boron positions*. Thus, for the section $\rho(x', y', 0)$ this series, in addition to reproducing the boron positions, gave no peaks at the hydrogen positions, but did reproduce the two close to the origin. The latter, then, appear to be a result of incompleteness of the Fourier series or some similar factor. The 14 hydrogen atoms are, then, located—at least approximately.

Of course, the resolution of the hydrogen atoms was not very fine, as would be expected, and it was not possible to obtain their parameters with great precision. The centers of the peaks were determined as well as possible, but were not always used for the parameters. Minor adjustments in their positions were made in some cases in order to make their disposition conform to the molecular symmetry $mm2$, given by the boron atoms, but keeping the distance from the bonded boron atom unchanged.

Background level

Aside from the peaks discussed above, the background did not exceed 0·3 e.A.$^{-3}$, and only rarely became as low as $-0·3$ e.A.$^{-3}$.

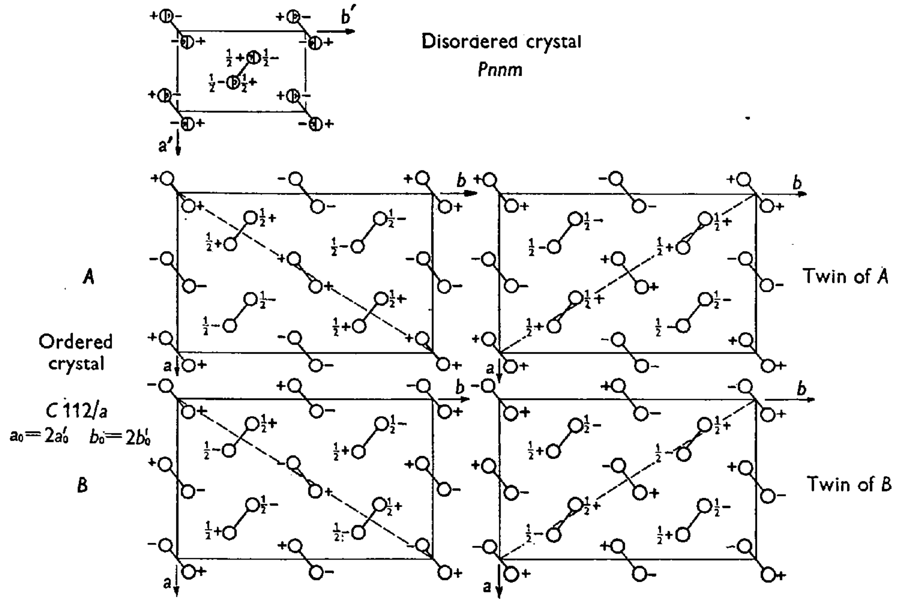

Fig. 7. Relation between disordered and ordered structures.

The final parameters for the *disordered* structure are:

	x'	y'	z
B_I	0·070	0·157	0·000
B_{II}	0·198	0·047	0·162
B_{III}	0·228	0·054	$-0·140$
B_{IV}	0·193	$-0·096$	0·000
B_V	0·039	$-0·081$	0·233
H_I	0·122	0·276	0·000
H_{II}	0·304	0·066	0·322
H_{III}	0·378	0·090	$-0·226$
H_{IV}	0·340	$-0·168$	0·000
H_V	0·076	$-0·156$	0·385
H_{VI}	0·088	0·136	$-0·231$
H_{VII}	0·188	$-0·070$	$-0·231$

Space group D_{2h}^{12}–$Pnnm$. All atoms in general positions 8 (h).

The ordered structure

Some general features of the ordered structure—particularly its space-group derivation—have already been outlined. We now turn to a full discussion of its solution, although this was done concurrently with the solution of the disordered structure.

The relation between the two is shown in Fig. 7. In accordance with the knowledge that the space group for the ordered crystal is $C\,112/a$, there are shown the two possible structures derivable from the disordered state. The notation used is that of the Space Group Tables in *Internationale Tabellen...* (1935, vol. 1), whereby a circle represents a general atom position. For our case, it is convenient also to consider it as representing the asymmetric unit of one half the $B_{10}H_{14}$ molecule. The difference between A and B is one of molecular geometry—the cap model for A, crown for B. In both cases the crystal would be monoclinic and a monoclinic axis is indicated in the diagram. The orthorhombic cell, because of its relation to the small cell of the disordered crystal ($a_0=2a_0'$, $b_0=2b_0'$), will be used, however. For A, the one which was established as correct, the symmetry center does not occur at the origin of the pictured cell.

The atomic positions and structure factors in the two cases follow:

A = Cap model (origin at center of symmetry)

Atoms at

$$\begin{array}{llll}
x,y,z & x,\tfrac{1}{2}+y,\bar{z} & \tfrac{1}{2}+x,y,\bar{z} & \tfrac{1}{2}+x,\tfrac{1}{2}+y,z \\
\bar{x},\bar{y},\bar{z} & \bar{x},\tfrac{1}{2}-y,z & \tfrac{1}{2}-x,\bar{y},z & \tfrac{1}{2}-x,\tfrac{1}{2}-y,\bar{z}
\end{array}$$

$$\begin{array}{ll}
\tfrac{1}{4}+x,-\tfrac{1}{4}-y,\tfrac{1}{2}-z & \tfrac{1}{4}-x,\tfrac{1}{4}+y,\tfrac{1}{2}-z \\
-\tfrac{1}{4}-x,\tfrac{1}{4}+y,\tfrac{1}{2}+z & -\tfrac{1}{4}+x,-\tfrac{1}{4}-y,\tfrac{1}{2}+z \\
\tfrac{1}{4}-x,-\tfrac{1}{4}+y,\tfrac{1}{2}+z & \tfrac{1}{4}+x,\tfrac{1}{4}-y,\tfrac{1}{2}+z \\
-\tfrac{1}{4}+x,\tfrac{1}{4}-y,\tfrac{1}{2}-z & -\tfrac{1}{4}-x,-\tfrac{1}{4}+y,\tfrac{1}{2}-z
\end{array}$$

where $x=\frac{1}{2}x'$, $y=\frac{1}{2}y'+\frac{1}{4}$, $z=z'$.

B = Crown model

Atoms at

$$\begin{array}{llll}
x,y,z & \tfrac{1}{2}+x,y,\bar{z} & \bar{x},\tfrac{1}{2}-y,z & \tfrac{1}{2}-x,\tfrac{1}{2}-y,\bar{z} \\
\bar{x},\bar{y},\bar{z} & \tfrac{1}{2}-x,\bar{y},z & x,\tfrac{1}{2}+y,\bar{z} & \tfrac{1}{2}+x,\tfrac{1}{2}+y,z
\end{array}$$

$$\begin{array}{ll}
\tfrac{1}{4}-x,\tfrac{1}{4}+y,\tfrac{1}{2}+z & \tfrac{3}{4}+x,\tfrac{1}{4}-y,\tfrac{1}{2}+z \\
\tfrac{1}{4}+x,\tfrac{1}{4}-y,\tfrac{1}{2}-z & \tfrac{3}{4}-x,\tfrac{1}{4}+y,\tfrac{1}{2}-z \\
\tfrac{1}{4}+x,\tfrac{3}{4}-y,\tfrac{1}{2}+z & \tfrac{3}{4}+x,\tfrac{3}{4}-y,\tfrac{1}{2}-z \\
\tfrac{1}{4}-x,\tfrac{3}{4}+y,\tfrac{1}{2}-z & \tfrac{3}{4}-x,\tfrac{3}{4}+y,\tfrac{1}{2}+z
\end{array}$$

where $x=\frac{1}{2}x'$, $y=\frac{1}{2}y'$, $z=z'$.

For both cases, the structure-factor equations are identical:

For h, k both even:

(1) $h+k+2l=4n$, $A=16\cos 2\pi hx \cos 2\pi ky \cos 2\pi lz$,

(2) $h+k+2l=4n+2$, $A=-16\sin 2\pi hx \sin 2\pi ky \cos 2\pi lz$.

For h, k both odd:

(1) $h+k+2l=4n$, $A=-16\sin 2\pi hx \cos 2\pi ky \sin 2\pi lz$,

(2) $h+k+2l=4n+2$, $A=-16\cos 2\pi hx \sin 2\pi ky \sin 2\pi lz$.

Thus, both A and B give identical intensities for h and k both even—the 'sharp reflections', which were used for the disordered structure. For h and k both odd, the difference in calculated values results from the one-quarter difference in y parameters.

The direct test of comparing calculated and observed $|F|$ values could not be made, since no crystals were ever found in the completely ordered state. Instead, the data available for making the distinction between A and B consist of the diffuse reflections for h, k odd, given by partially ordered structures. It is necessary, therefore, to consider the manner in which the disordering arises.

The partially ordered crystal

Referring to the cells for the ordered structure in Fig. 7, it can be seen that for either A or B there are two arrangements of molecules, or 'twins', which give identical diffraction effects. It is most convenient to consider them in terms of the x, z planes of molecules. For both twins, the sequence of second layers is the same, although they differ in respect to pairing of adjacent layers. Referring to Fig. 8, where the boron framework of the projected molecule is outlined (cap model), the one twin can be described as formed by the sequence *ACBD* of the x, z layers, the sequence being *ADBC* for the other. On this basis, a qualitative explanation suggests itself for the experimental observations pertaining to the partially ordered state. Both the diffuseness of only those reflections with h, k odd and the streaking in the $\mathbf{b}^*$ direction can be expected from a mixing of the two sequences, subject to the condition that an A or B layer is always followed by only C or D. The situation in the actual crystals studied may be pictured as follows:

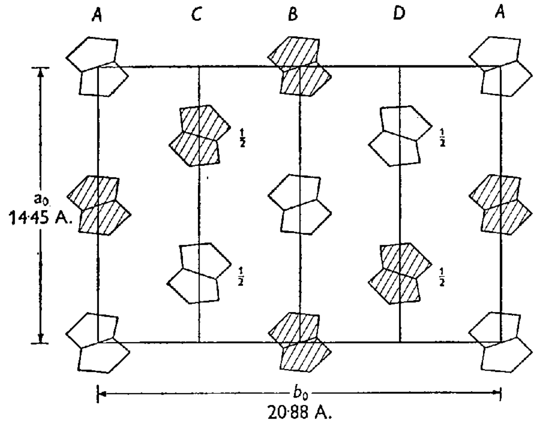

Fig. 8. Unit cell of ordered structure illustrating arrangement of x, z layers for one twin of cap model, A. Molecules are outlined by projected boron positions. The edge common to both halves of a molecule is at positive z values for a non-shaded figure, and at negative values for a shaded one.

ACBDACBD...ACBDADBCADBC...ADBCBCAD...

A quantitative treatment of the disordering phenomenon similar to the methods worked out by Hendricks & Teller (1942) for layer structures has been made. It will not be given in detail here, since it is to be the subject of a separate paper. It was assumed that the four layers occur with equal frequency and that correlation exists between neighboring layers only, corresponding to the condition above. An expression was obtained for the average intensity per layer in terms of a parameter expressing the probability for any two layers occurring as jth neighbors and serving, consequently, as a measure of the extent of disorder. This parameter could be evaluated from the variation of intensity along a streak in the **b*** direction. As a crude estimate, it was found that the amount of disorder in the crystals studied corresponded to a probability of 1/20 that a specific layer had the same kind of layer as a second neighbor. Also in other respects, the results of this treatment were in agreement with the observed diffraction effects.

Intensities of the diffuse reflections

In terms of the amplitude expressions, given above, for the ordered structure, the measured intensities of 'diffuse reflections' represent averaged quantities. Thus, at the reciprocal-lattice points hkl and $\bar{h}\bar{k}l$ (h, k both odd), the intensity is proportional to $\frac{1}{2}(F^2_{hk} + F^2_{\bar{h}\bar{k}l})$. In all cases observed the intensities were the same at each of the points of reciprocal space corresponding to the various planes of the same form. This is in accordance with the assumption above that all four types of x, z layers occur with equal frequency.

These were the quantities—$\frac{1}{2}(F^2_{hkl} + F^2_{\bar{h}\bar{k}l})$—that were calculated and compared with the intensities in deciding between the cap and crown models. The measured intensity values were placed on an 'absolute basis' by application of the same factors that had been used for the sharp reflections. Although these resultant values could be expected to be too low (in terms of electrons), since only the maximum intensity at the reciprocal lattice point for a diffuse streak was estimated and not the fully integrated intensity, the observed and calculated numbers were almost on the same basis, and no further adjustment by a scale factor was made. In Table 11 the calculated '$|F_{hkl}|$' is the averaged term, $|\overline{F_{hkl}}| = \sqrt{\{\frac{1}{2}(F^2_{hkl} + F^2_{\bar{h}\bar{k}l})\}}$, for reflections with h and k odd.

On the average, the magnitude of the 'diffuse' intensities is considerably smaller than for the sharp reflections. Only a fraction of the total number of atoms contributes to these intensities—three boron and five hydrogen atoms of the asymmetric unit. The structure factors (cf. above) contain the term $\sin 2\pi lz$ and thus B_{I}, B_{IV}, H_{I} and H_{IV}, for which $z = 0$, have no contribution. Also, the contributions of B_{II} and B_{III} generally cancel each other to a large extent, because of the close overlap of these atoms upon reflection through $z = 0$.

For high values of $(\sin\theta)/\lambda$ ($> 0{\cdot}5$) the search for, and intensity estimation of, the weak diffuse streaks was a difficult and lengthy procedure. The numbers obtained, therefore, cannot be expected to be of great precision. Nonetheless, the agreement with calculated values for the cap model was, on the whole, better than expected.

Fourier syntheses

To test the validity of the conclusions about the ordered structure, more than to obtain parameter values, Fourier syntheses were undertaken. For this, an assumption had to be made regarding the individual values, F_{hkl} against $F_{h\bar{k}l}$, since only the average of their squares was observed. Accordingly, the observed term $|\overline{F_{hkl}}|^2$ was split into two parts, $|F_{hkl}|^2$ and $|F_{\bar{h}\bar{k}l}|^2$, in proportion to the ratio of the corresponding calculated quantities, which also provided the proper signs.

The entire large cell was explored in the same manner as the small cell (parallel sections, perpendicular to **c**, spaced 0·19 A. apart). The section $\rho(x, y, 0)$ is, of course, the same as for the small cell—only the F's for sharp reflections enter into it. In view of the imperfect nature of the diffuse-diffraction data, the results were satisfactory. The separation of the molecule from its image, which is effected only by the F's with h, k odd, was accomplished, although not completely. In some cases, 'ghosts', in positions $x, y, \bar{z}$, were observed for atoms at x, y, z. For example, symmetrical to B_{V}, which had a peak electron density of ~ 4 e.A.$^{-3}$, there was a peak of ~ 1 e.A.$^{-3}$. This result was not surprising. In other respects, the structure indicated by the three-dimensional syntheses conformed to that already deduced for the ordered crystal. The boron parameters deduced were the same as those previously used, and all hydrogen peaks were present in the proper positions.

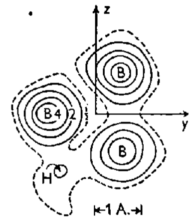

Fig. 9. Section at $x = 0{\cdot}1$.

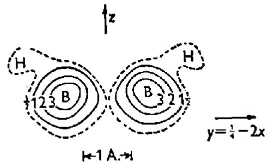

Fig. 10. Section on transverse mirror plane of molecule.

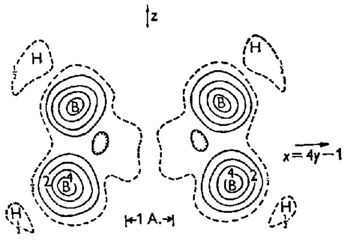

Fig. 11. Section on longitudinal mirror plane of molecule.

Views of the electron contours delineating hydrogen atoms in the neighborhood of boron atoms are given in Figs. 9, 10 and 11. The sections shown are for the two mirror planes of the molecule, and also for the plane including B_{II}, B_{III}, B_{IV} and the bridge hydrogen H_{VII}.

No attempt was made to change the parameters used for the F calculations prior to the Fourier syntheses. They were obtained from those for the disordered structure by the relations, $x = \frac{1}{2}x'$, $y = \frac{1}{2}y' + \frac{1}{4}$, $z = z'$.

The general positions are those given in the first part of this section for the cap model.

Reliability of the structure

The comparison of observed and calculated* $|F|$'s is made in Tables 10 and 11. All $|F|$'s are included, for both sharp and diffuse reflections. For the latter, however, the $|F|$ is the averaged quantity mentioned previously. The sharp reflections are given the indices appropriate to the large cell. The Hartree atomic scattering factors for boron and hydrogen, given in *Internationale Tabellen...* (1935, vol. 2, p. 571), were used in the calculations. A temperature-factor correction was applied, which on the assumption of spherical atoms corresponds to a value for B in $\exp[-B\{(\sin\theta)/\lambda\}^2]$ of 3·5 A.^{2}.

It is believed that the agreement of the observed and calculated $|F|$'s is more than satisfactory. The usual index of reliability, $\Sigma[|F|_{\text{obs.}} - |F|_{\text{calc.}}]/\Sigma|F|_{\text{obs.}}$, for all *sharp* reflections, was 0·19 if calculated values for non-observed reflections were excluded and 0·25 with their inclusion. The index for other selected groups of reflections was:

$$hk0 \quad 0{\cdot}22 \qquad h0l \quad 0{\cdot}25 \qquad 0kl \quad 0{\cdot}21$$

with inclusion of calculated values for non-observed reflections. These numbers compare favorably with those obtained in many structure determinations free of the many complications involved here. It is to be noted that certain factors responsible for significantly lower values of the index in other cases could not be appropriately ascertained for $B_{10}H_{14}$. Undoubtedly, the assumption of spherical atoms is not completely valid—there were indications in the contour maps of preferred directions of concentration of the electron density about a boron peak—but it was not possible to allow for this quantitatively. Also, there are no previous experimental data as to the proper scattering factors for a boron hydride—the Hartree functions may not be the most suitable. It must be remembered, too, that the hydrogen share of the total number of electrons ($\frac{14}{64}$) is considerable.

The large individual discrepancies in the $|F|$ values are understandable for the most part. The first five reflections in order of $(\sin\theta)/\lambda$ were observed much weaker than calculated. This not uncommon situation is an indication of large extinction effects, which cannot be readily allowed for. Attempts to obtain reliable intensity data for these reflections from powder patterns were unsuccessful. Owing to the volatility of the compounds, sublimation and recrystallization could not be prevented, even with closely packed powders in sealed-off capillaries, and spottiness in the diffraction rings was always obtained.

In several instances, no diffuse streak was observed where the calculated $|F|$ is appreciable. This generally applies to reflections for high $(\sin\theta)/\lambda$, and may result from the experimental difficulties of observation discussed previously. The labor required to reinvestigate all regions where it was difficult to ascertain the presence of a diffuse streak, particularly those corresponding to edges of films, seemed prohibitive.

Otherwise, the discrepancies may be ascribed to the factors already mentioned.

Table 10. *Comparison of $F_{\text{calc.}}$ and $F_{\text{obs.}}$ for sharp reflections*

hkl	$F_{\text{calc.}}$	$F_{\text{obs.}}$	*hkl*	$F_{\text{calc.}}$	$F_{\text{obs.}}$	*hkl*	$F_{\text{calc.}}$	$F_{\text{obs.}}$
400	−52	39	880	+ 2	<5	4,18,0	+19	25
800	+25	35	10,8,0	+ 9	14	6,18,0	− 2	<9
12,0,0	− 7	8	12,8,0	+ 2	<5	8,18,0	+ 1	<7
16,0,0	−17	13	14,8,0	+11	13	10,18,0	+ 2	<4
220	−123	54	2,10,0	+25	34	0,20,0	−15	12
420	+19	19	4,10,0	−10	12	2,20,0	− 2	<8
620	+26	29	6,10,0	− 7	9	4,20,0	+ 6	<8
820	+11	20	8,10,0	−41	38	6,20,0	− 2	<7
10,2,0	−37	35	10,10,0	+17	21	8,20,0	− 4	<4
12,2,0	− 2	<5	12,10,0	+ 4	<5	2,22,0	− 3	<6
14,2,0	+24	28	14,10,0	− 4	4	4,22,0	− 6	<5
16,2,0	− 6	4	0,12,0	−38	44	201	+78	46
040	+112	69	2,12,0	−41	43	601	−35	31
240	−20	24	4,12,0	+23	22	10,0,1	+22	29
440	−63	48	6,12,0	+36	31	14,0,1	−22	26
640	+ 2	5	8,12,0	−18	18	021	−135	69
840	+31	30	10,12,0	− 2	<5	221	+10	9
10,4,0	−10	12	12,12,0	−10	12	421	+44	39
12,4,0	+ 5	<5	2,14,0	+ 6	<8	621	+28	32
14,4,0	+14	17	4,14,0	+32	25	821	−14	22
260	+31	27	6,14,0	− 8	10	10,2,1	+16	24
460	−27	32	8,14,0	−14	14	12,2,1	+ 2	6
660	+23	27	10,14,0	+21	24	14,2,1	− 5	<4
860	−13	16	12,14,0	+19	20	241	+ 1	7
10,6,0	−21	25	0,16,0	−34	28	441	−19	20
12,6,0	− 4	11	2,16,0	−37	32	641	−24	28
14,6,0	− 3	<5	4,16,0	+13	14	841	−25	29
080	−59	45	6,16,0	− 3	<9	10,4,1	+23	25
280	−34	36	8,16,0	−13	13	12,4,1	− 2	7
480	−21	26	10,16,0	−12	17	14,4,1	− 5	5
680	+48	43	2,18,0	+14	17	061	+21	22

---

* The final calculations of F's were made with IBM machines by the method described by Grems & Kasper (1949).

Table 10 (*cont.*)

hkl	$F_{\text{calc.}}$	$F_{\text{obs.}}$
261	−4	<3
461	+25	25
661	−4	10
861	−10	14
10.6.1	+10	17
12.6.1	−6	<5
14.6.1	−7	10
281	−18	19
481	+17	20
681	+2	10
881	+16	16
10.8.1	−2	<5
12.8.1	+1	<5
14.8.1	+6	6
0.10.1	+24	24
2.10.1	+15	18
4.10.1	−17	18
6.10.1	−33	33
8.10.1	+7	<5
10.10.1	−6	<5
12.10.1	+5	9
14.10.1	−2	<2
2.12.1	+3	<5
4.12.1	−7	8
6.12.1	+21	23
8.12.1	+22	23
10.12.1	−18	22
12.12.1	−9	11
0.14.1	+7	8
2.14.1	+31	29
4.14.1	−21	20
6.14.1	−6	8
8.14.1	+10	9
10.14.1	+6	10
12.14.1	+5	<3
2.16.1	−3	<5
4.16.1	−24	27
6.16.1	+4	<5
8.16.1	+4	<5
10.16.1	−5	<4
0.18.1	+16	14
2.18.1	+14	13
4.18.1	0	<5
6.18.1	+1	<5
8.18.1	+3	<4
2.20.1	−6	<8
4.20.1	+2	<7
6.20.1	−3	<6
0.22.1	+1	<5
2.22.1	−8	5
4.22.1	−1	<5
002	+3	7
402	−10	16
802	−17	8
12.0.2	−4	10
222	+9	12
422	+21	20
622	+16	20
822	+32	29
10.2.2	+5	6
12.2.2	+2	<4
14.2.2	+3	<3
042	−52	42
242	+30	26
442	−10	15
642	−40	35
842	−4	<5
10.4.2	−24	24
12.4.2	+4	<5
14.4.2	−1	<5
262	+23	26
462	−5	7
662	−1	<5
862	+36	31
10.6.2	+1	<6
12.6.2	−1	<5
14.6.2	−10	5
082	−21	24
282	+26	24
482	+16	18
682	−12	12
882	+1	<6
10.8.2	−2	8
12.8.2	+1	<5
14.8.2	−1	<2
2.10.2	−11	13
4.10.2	−13	12
6.10.2	−27	28
8.10.2	+2	7
10.10.2	+8	14
12.10.2	−4	7
0.12.2	+27	28
2.12.2	+5	<9
4.12.2	+29	25
6.12.2	+1	<9
8.12.2	+4	7
10.12.2	+3	<4
12.12.2	−8	9
2.14.2	−22	24
4.14.2	+8	6
6.14.2	−12	14
8.14.2	−2	<5
10.14.2	+2	<4
0.16.2	+15	17
2.16.2	−10	10
4.16.2	−1	<9
6.16.2	+2	<9
8.16.2	+5	<8
10.16.2	+1	<4
2.18.2	+3	<9
4.18.2	+2	<8
6.18.2	+9	<7
8.18.2	−6	<5
0.20.2	+3	<7
2.20.2	+2	<7
4.20.2	−15	10
6.20.2	+8	<4
2.22.2	+2	<4
203	+13	14
603	+8	13
10.0.3	−18	16
14.0.3	0	<2
023	+14	17
223	−16	18
423	−20	19
623	+28	28
823	+16	14
10.2.3	+8	13
12.2.3	−1	<5
14.2.3	−2	<2
243	−19	20
443	+6	9
643	+9	10
843	−40	32
10.4.3	−8	8
12.4.3	+9	8
063	+49	38
263	−45	33
463	−9	11
663	+29	25
863	+5	9
10.6.3	+2	<5
12.6.3	−6	5
283	−15	15
483	+27	23
683	+13	16
883	−20	20
10.8.3	−7	11
12.8.3	+15	19
0.10.3	+8	<6
2.10.3	−33	24
4.10.3	−16	16
6.10.3	+8	10
8.10.3	0	<6
10.10.3	−10	13
12.10.3	+5	6
2.12.3	+13	14
4.12.3	+10	5
6.12.3	+11	14
8.12.3	−6	<6
10.12.3	−6	9
0.14.3	−22	19
2.14.3	−5	<9
4.14.3	−2	<9
6.14.3	+10	11
8.14.3	−4	4
10.14.3	−1	<2
2.16.3	+5	<9
4.16.3	−7	6
6.16.3	−8	3
8.16.3	−4	<3
0.18.3	−12	9
2.18.3	+3	<7
4.18.3	+19	13
6.18.3	+1	<4
2.20.3	−1	<4
004	+29	29
404	+30	28
804	−7	8
12.0.4	+1	8
224	−20	23
424	+1	<5
624	−11	14
824	+15	15
10.2.4	+3	<5
12.2.4	−6	7
044	−13	9
244	+25	24
444	+14	16
644	−21	22
844	−3	7
10.4.4	+1	6
12.4.4	+5	<3
264	+15	14
464	−21	21
664	−5	<5
864	+13	13
10.6.4	+2	<4
084	−31	25
284	+34	28
484	+2	<5
684	−3	<5
884	−3	7
10.8.4	+14	21
2.10.4	+11	9
4.10.4	−20	16
6.10.4	−4	5
8.10.4	−2	7
10.10.4	+9	9
0.12.4	−4	<9
2.12.4	+13	6
4.12.4	−1	<5
6.12.4	−3	<5
8.12.4	−2	4
2.14.4	0	<8
4.14.4	+6	7
6.14.4	+4	5
0.16.4	+6	<6
2.16.4	−6	6
4.16.4	−12	6
205	+21	25
605	−4	9
025	−22	24
225	−3	<5
425	−1	7
625	+9	11
825	0	6
245	+1	<5

Table 10 (*cont.*)

hkl	$F_{\text{calc.}}$	$F_{\text{obs.}}$	*hkl*	$F_{\text{calc.}}$	$F_{\text{obs.}}$	*hkl*	$F_{\text{calc.}}$	$F_{\text{obs.}}$
445	+ 1	< 5	685	+ 1	< 3	2,14,5	+ 7	< 4
645	− 3	7	885	+ 4	3	006	+20	19
845	− 9	10	0,10,5	+ 9	8	406	−14	18
065	+12	13	2,10,5	− 4	< 7	226	− 3	3
265	−10	12	4,10,5	− 3	< 3	426	+ 5	7
465	+ 4	5	6,10,5	− 6	7	046	+ 5	4
665	+ 3	6	2,12,5	0	< 3	246	− 4	4
865	− 1	< 3	4,12,5	− 1	< 3	446	−12	12
285	−10	7	0,14,5	0	< 4	266	+ 5	4
485	+ 9	7						

Table 11. *Comparison of* $F_{\text{calc.}}$ *and* $F_{\text{obs.}}$ *for diffuse reflections*

$$F_{\text{calc.}} = \sqrt{\{\tfrac{1}{2}(F^2_{hkl}+F^2_{\bar{h}\bar{k}l})\}}$$

hkl	$F_{\text{calc.}}$	$F_{\text{obs.}}$	*hkl*	$F_{\text{calc.}}$	$F_{\text{obs.}}$	*hkl*	$F_{\text{calc.}}$	$F_{\text{obs.}}$
111	33	16	7,17,1	3	< 8	7,15,2	3	< 9
311	34	18	9,17,1	2	< 6	9,15,2	3	< 7
511	16	11	1,19,1	2	< 9	1,17,2	2	< 9
711	9	7	3,19,1	4	< 9	3,17,2	4	< 9
911	6	7	5,19,1	3	< 8	5,17,2	2	< 9
11,1,1	9	7	7,19,1	4	< 6	7,17,2	3	< 7
13,1,1	5	< 5	1,21,1	3	< 7	1,19,2	2	< 8
15,1,1	5	< 3	3,21,1	3	< 6	3,19,2	3	< 8
131	24	11	5,21,1	3	< 5	5,19,2	0	< 7
331	24	14	112	5	4	1,21,2	2	< 5
531	16	12	312	11	9	3,12,2	2	< 5
731	15	14	512	3	6	113	13	10
931	13	11	712	7	7	313	9	8
11,3,1	11	10	912	5	< 5	513	6	5
13,3,1	4	< 7	11,1,2	8	6	713	11	9
15,3,1	4	< 3	13,1,2	5	< 4	913	8	9
151	13	6	132	4	4	11,1,3	1	< 5
351	9	7	332	11	7	13,1,3	3	< 3
551	11	7	532	6	8	133	13	11
751	17	15	732	7	7	333	7	< 4
951	16	13	932	5	< 5	533	7	8
11,5,1	13	12	11,3,2	7	8	733	12	10
13,5,1	4	< 8	13,3,2	4	< 4	933	7	7
171	2	< 2	152	7	5	11,3,3	3	< 7
371	4	6	352	8	7	13,3,3	4	< 3
571	7	8	552	6	7	153	9	8
771	14	13	752	6	7	353	3	< 4
971	16	11	952	6	< 5	553	9	7
11,7,1	12	9	11,5,2	6	< 5	753	13	11
13,7,1	2	< 8	13,5,2	3	< 7	953	7	6
191	6	7	172	7	6	11,5,3	4	< 8
391	12	9	372	3	5	13,5,3	5	< 3
591	9	10	572	6	5	173	3	5
791	11	14	772	4	< 5	373	2	6
991	13	13	972	8	8	573	9	8
11,9,1	9	5	11,7,2	6	5	773	12	10
13,9,1	0	< 7	13,7,2	3	< 6	973	6	9
1,11,1	11	5	192	5	4	11,7,3	3	< 8
3,11,1	15	11	392	3	5	193	6	< 8
5,11,1	12	9	592	6	< 4	393	7	9
7,11,1	8	< 5	792	3	7	593	8	8
9,11,1	8	7	992	9	7	793	10	11
11,11,1	5	< 5	11,9,2	5	< 5	993	4	11
13,11,1	2	6	13,9,2	3	< 4	11,9,3	2	< 6
1,13,1	11	< 9	1,11,2	2	< 8	1,11,3	11	< 9
3,13,1	15	3	3,11,2	6	6	3,11,3	9	< 9
5,13,1	11	9	5,11,2	6	7	5,11,3	7	< 5
7,13,1	5	< 5	7,11,2	1	< 5	7,11,3	7	< 6
9,13,1	4	6	9,11,2	7	6	9,11,3	3	6
11,13,1	2	6	11,11,2	3	< 4	11,11,3	1	< 3
1,15,1	9	< 9	1,13,2	1	< 9	1,13,3	11	< 9
3,15,1	11	< 9	3,13,2	7	< 9	3,13,3	8	< 9
5,15,1	8	5	5,13,2	6	10	5,13,3	5	< 6
7,15,1	3	< 5	7,13,2	2	12	7,13,3	5	< 7
9,15,1	0	< 8	9,13,2	5	< 5	9,13,3	4	< 4
11,15,1	4	< 5	11,13,2	2	4	1,15,3	9	< 9
1,17,1	5	< 9	1,15,2	1	< 9	3,15,3	5	< 9
3,17,1	6	< 9	3,15,2	6	< 9	5,15,3	3	8
5,17,1	5	< 9	5,15,2	4	< 9	7,15,3	4	< 7

Table 11 (*cont.*)

$F_{\text{calc.}}=\sqrt{\{\tfrac{1}{2}(F^2_{hkl}+F^2_{h\bar{k}l})\}}$

hkl	$F_{\text{calc.}}$	$F_{\text{obs.}}$	*hkl*	$F_{\text{calc.}}$	$F_{\text{obs.}}$	*hkl*	$F_{\text{calc.}}$	$F_{\text{obs.}}$
1,17,3	5	< 8	574	3	< 5	915	3	< 3
3,17,3	2	< 8	774	6	5	135	4	5
5,17,3	2	< 7	974	5	6	335	4	< 5
1,19,3	1	< 6	194	1	< 8	535	5	< 8
3,19,3	2	< 5	394	4	7	735	6	< 6
114	8	6	594	3	< 6	155	2	< 5
314	5	< 5	794	5	< 4	355	2	6
514	2	< 5	994	5	< 3	555	5	6
714	2	< 5	1,11,4	3	< 9	755	5	< 6
914	4	< 5	3,11,4	5	7	175	1	< 8
11,1,4	4	< 3	5,11,4	3	< 8	375	2	< 6
134	6	11	7,11,4	3	< 4	575	5	< 6
334	4	< 5	9,11,4	4	5	775	4	5
534	2	6	1,13,4	3	< 9	195	4	< 8
734	4	< 9	3,13,4	5	8	395	3	6
934	5	< 5	5,13,4	2	5	595	4	4
11,3,4	4	5	7,13,4	2	< 3	1,11,5	5	< 7
154	4	< 5	1,15,4	3	< 7	3,11,5	4	3
354	2	< 5	3,15,4	4	< 7	5,11,5	4	< 3
554	2	< 5	5,15,4	1	< 3	1,13,5	5	< 5
754	5	6	1,17,4	3	< 5	116	5	7
954	5	< 8	115	5	6	316	1	3
11,5,4	3	< 3	315	4	< 6	136	4	4
174	2	< 5	515	5	5			
374	3	< 5	715	7	6			

Interatomic distances

From the final set of parameters, the following interatomic distances within the decaborane molecule were obtained:

B_I–B_{II}	1·74 ± 0·03 A.	B_I–H_I	1·26 A.
B_I–B_{III}	1·76 ± 0·03	B_{II}–H_{II}	1·29
B_I–B'_V	1·74 ± 0·02	B_{III}–H_{III}	1·25
B_{II}–B_{III}	1·73 ± 0·04	B_{IV}–H_{IV}	1·29
B_{II}–B_{IV}	1·76 ± 0·03	B_V–H_V	1·28
B_{II}–B_V	1·81 ± 0·04		
B_{II}–B'_V	1·79 ± 0·04	B_I–H_{VI}	1·34
B_{III}–B_{IV}	1·78 ± 0·03	B_{III}–H_{VI}	1·40
B_{IV}–B_V	1·74 ± 0·02	B_{IV}–H_{VII}	1·34
B_V–B'_V	1·78 ± 0·02	B_{III}–H_{VII}	1·40
B_I–B'_{IV} B'_I–B_{IV}	2·01 ± 0·02		

The limits of error are conservatively set on the basis of the estimated uncertainties of the respective parameters, which are of varying degrees of reliability. It is considerably more difficult to fix the limits of error on hydrogen parameters, but it would appear that the boron–hydrogen *distances* are probably correct to about ± 0·05 A.

Taking into account these distances, and referring to Figs. 6 and 12, a better description of the molecule can now be given. The boron framework consists of two almost regular pentagonal pyramids sharing an edge (B_V–B'_V) with an angle of 76° between the base planes of the pyramids ($\angle B_I$–B'_V–B'_{IV}). There are two additional longer bonds of 2·01 A. joining the pyramids. It is not possible to say whether the differences in the distances within the pyramid are real. Accepting an overall average of 1·77 A., one can say they are equal within ± 0·04 A.

The surface of the molecule consists entirely of hydrogen atoms. The ten regular ones each joined singly to a boron atom at distances of 1·25–1·29 A. are in directions roughly corresponding to fivefold axes of the distorted icosahedral figure suggested by the boron atoms. The angles of these B–H bonds to adjacent B–B bonds vary between 110 and 134°.

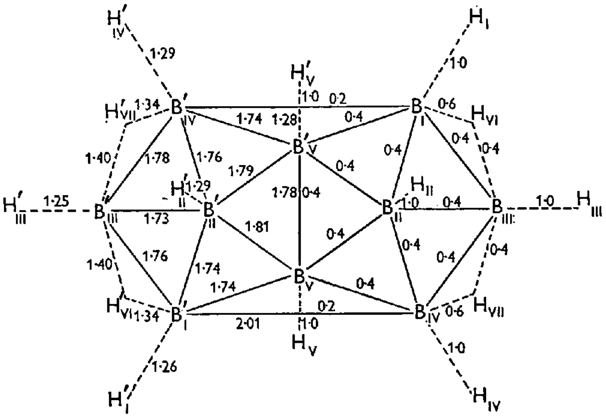

Fig. 12. Topological diagram with bond lengths (on left) and bond numbers (on right).

The bridging hydrogen atoms seem now to be in reasonable positions, in that they complete the surface of the molecule outlined by the other hydrogen atoms and also make the co-ordination number of each boron 6. That they are unsymmetrically placed with respect to the two bonding boron atoms is not too surprising, since the longer leg of the bridge is to B_{III} which is bound to two such hydrogen atoms.

The closest approach of hydrogen atoms within the molecule is 1·98 A. The intermolecular contacts are all through hydrogen atoms, and the shortest distances are in the range 2·5–3·0 A.

Chemical implications

In attempting to understand the strange structure of the molecule and the peculiar bonding within it, the most successful interpretation has been in terms of resonating single bonds, such as used by Pauling (1947) in describing metallic binding.

In Fig. 12 there are given (in addition to the bond distances) bond numbers, as defined by Pauling. They have not been derived from the equation of Pauling relating bond number to interatomic distance, but as follows. Each of the regular B–H's is considered to be a full covalent bond and hence of bond number 1. Four boron atoms (B_{II}, B'_{II}, B_V, B'_V) then each have five equivalent bonds to boron, among which two electrons are to be distributed. These bonds are consequently assigned a bond number of 0·4. In order to keep the valence of B_{III} at three, the longer legs of the hydrogen bridges would need to be of bond number 0·4—this in turn makes the bond number for the shorter legs 0·6 and for the long B–B bond 0·2. In other words, with this assignment of bond numbers each boron is trivalent and each hydrogen monovalent. The relation used by Pauling is $R(1)-R(n)=0{\cdot}3\log n$, where n is the bond number, and $R(1)$ and $R(n)$ are respectively the radius for a single covalent bond and for one of bond number n. From this relation the value of $R(1)$ is 0·77 A. if calculated from the B–B bonds of 1·77 and 0·80 A. from the long bond of 2·01 A. The value given by Pauling is 0·80 A.

Although this description may not be the best one, it is rather definite that the binding within the molecule is of the 'metallic' type with a mobile system of electrons, and for which the bonds have directional properties different from those ascribed to normal covalent linkages.

We acknowledge with pleasure the very capable assistance in the work of Mrs J. Belanger and of Miss M. D. Grems, and are grateful to Dr A. L. Marshall for his enthusiastic interest in and support of this research.

This work was performed under U.S. Army Ordnance Contract TUI-2000.

References

Bragg, W. L. (1929). *Z. Krystallogr.* **70**, 475.
Buerger, M. J. (1947). *J. Chem. Phys.* **15**, 1.
Gillis, J. (1948*a*). *Acta Cryst.* **1**, 76.
Gillis, J. (1948*b*). *Acta Cryst.* **1**, 174.
Grems, M. D. & Kasper, J. S. (1949). *Acta Cryst.* **2**, 347.
Harker, D. (1948). *Amer. Min.* **33**, 764.
Harker, D. & Kasper, J. S. (1948). *Acta Cryst.* **1**, 70.
Hendricks, S. & Teller, E. (1942). *J. Chem. Phys.* **10**, 147.
Huggins, M. L. (1941). *J. Amer. Chem. Soc.* **63**, 66.
Internationale Tabellen zur Bestimmung von Kristallstrukturen (1935). Berlin: Borntraeger.
Kasper, J. S., Lucht, C. M. & Harker, D. (1948). *J. Amer. Chem. Soc.* **70**, 881.
Mark, H. & Pohland, E. (1925). *Z. Krystallogr.* **62**, 103.
Möller, H. (1931). *Z. Krystallogr.* **76**, 500.
Pauling, L. (1947). *J. Amer. Chem. Soc.* **69**, 542.
Roth, W. L. & Harker, D. (1948). *Acta Cryst.* **1**, 34.
Shaffer, P. H., Schomaker, V. & Pauling, L. (1946). *J. Chem. Phys.* **14**, 648.
Stock, A. & Pohland, E. (1928). *Ber. dtsch. chem. Ges.* **62**, 90.
Wilson, A. J. C. (1942). *Nature, Lond.*, **150**, 152.

Acta Cryst. (1950). **3**, 455

The Probability Distribution of X-ray Intensities. IV. New Methods of Determining Crystal Classes and Space Groups

By D. Rogers

Viriamu Jones Laboratory, University College, Cardiff, Wales

(*Received* 8 *April* 1950)

The application of the two methods of intensity statistics, the 'distribution method' and the 'method of averages', to the identification of the symmetry elements in a crystal is discussed. It is shown that each symmetry element has a distinct and recognizable effect on the weighted reciprocal lattice, and it is concluded that, from X-ray intensities alone, each crystal class may theoretically be identified uniquely. As a result 215 of the 219 space groups are also by these methods uniquely identifiable from X-ray data. Information concerning symmetry elements may also be obtained which is of value in structural investigations. A brief consideration is given to the remaining two pairs of space groups $I222$, $I2_12_12_1$ and $I23$, $I2_13$.

1. Introduction

The recent theoretical work on X-ray intensity statistics (Wilson, 1949, 1950) has shown that, except in certain foreseeable cases, the distribution of the structure amplitudes of the reflexions should conform to one or other of two Gaussian types. When the structure